The Geometrical Influence of Solid-State Ion-Pair Interactions of Alkali Metal Ions with a Binuclear Iron Acyl Monoanion, $[Fe_2(CO)_5(C(O)R)(\mu_2\text{-}PPh_2)_2]^-$ (Where R = Ph, Me). Structural Analyses of the $[Li(THF)_3]^+$, $[Na(THF)_2]^+$, and $[(Ph_3P)_2N]^+$ Salts

Robert E. Ginsburg,[1a] Jeremy M. Berg,[1b] Richard K. Rothrock,[1b,c] James P. Collman,[1b] Keith O. Hodgson,[1b] and Lawrence F. Dahl*[1a]

Contribution from the Departments of Chemistry, University of Wisconsin—Madison, Madison, Wisconsin 53706, and Stanford University, Stanford, California 94305.
Received February 12, 1979

Abstract: X-ray diffraction studies of the acyl $[Fe_2(CO)_5(C(O)R)(\mu_2\text{-}PPh_2)_2]^-$ monoanion, as the $[Na(THF)_2]^+$ and $[(Ph_3P)_2N]^+$ salts for R = Me and as the $[Li(THF)_3]^+$ salt for R = Ph, have established the binuclear iron monoanion to be geometrically analogous to the (Fe-Fe)-bonded $Fe_2(CO)_6(\mu_2\text{-}PPh_2)_2$ molecule with an equatorial carbonyl ligand formally replaced by a negatively charged acyl ligand. This structural investigation involving three widely differing counterions has also enabled a direct assessment of the type and extent of ion pairing of alkali metal ions with a metal acyl carbonylate anion in the solid state. The occurrence of tight ion pairing between the alkali metal and the acyl oxygen atom is found in both the $[Li(THF)_3]^+$ and $[Na(THF)_2]^+$ salts. The Li^+ ion possesses a nearly regular tetrahedral oxygen environment of one O(acyl) and three O(THF) atoms, while the Na^+ ion has a highly distorted square-pyramidal oxygen environment comprised of the O(acyl) atom and one O(carbonyl) atom from one monoanion, an O(carbonyl) atom from a symmetry-related monoanion, and two O(THF) atoms. An analysis reveals that the nature of interaction of the oxygen atom of a terminal acyl ligand with an alkali metal ion is completely different from its well-established interactions with either an R^+ substituent (carbene formation) or a second metal atom (acyl-bridged formation). In sharp contrast to the resulting in-plane (acyl) covalent bond between an O(acyl) atom and either a carbon or metal atom, geometrical evidence is presented in favor of the tight ion-pairing interaction between the terminal acyl ligand and the out-of-plane Li^+ or Na^+ ion involving primarily a charge polarization of the O(acyl) atom. A systematic correlation of the solid-state structural features of the binuclear iron acyl monoanion for the $[Li(THF)_3]^+$ salt with those of metal acyl complexes without ion pairing as well as with those of metal carbene complexes and of two binuclear metal acyl-bridged complexes has revealed geometrical trends. Bonding and stereochemical implications are also presented. $[(Ph_3P)_2N]^+[Fe_2(CO)_5(C(O)Me)(\mu_2\text{-}PPh_2)_2]^-$ crystallizes in an orthorhombic unit cell with dimensions a = 14.725 (4) Å, b = 11.608 (6) Å, c = 17.387 (5) Å; d_{calcd} = 1.32 g/cm^3 for Z = 2. The space-group symmetry $P2_122_1$ necessitates crystallographic C_2-2 site symmetry for both the cation and monoanion. The monoanion thereby possesses a crystallographic disorder between two orientations such that the equatorial acyl ligand of one Fe atom and an equatorial carbonyl ligand of the other Fe atom are nearly superimposed in the twofold-averaged crystal structure. Least-squares refinement gave $R_2(F)$ = 6.6% and $R_2(F)$ = 7.2% for 1213 reflections with $I \geq 2\sigma(I)$. $[Na(C_4H_8O)_2]^+[Fe_2(CO)_5(C(O)Me)(\mu_2\text{-}PPh_2)_2]^-$ crystallizes in a monoclinic unit cell of dimensions a = 9.284 (7) Å, b = 23.889 (21) Å, c = 18.427 (14) Å, β = 99.45 (6)°, and symmetry $P2_1/n$; d_{calcd} = 1.37 g/cm^3 for Z = 4. The structural determination was complicated by a crystal disorder of one THF molecule between two sites. Least-squares refinement yielded $R_1(F)$ = 12.9% and $R_2(F)$ = 11.4% for 1708 reflections with $I \geq 2\sigma(I)$. $[Li(C_4H_8O)_3]^+[Fe_2(CO)_5(C(O)Ph)(\mu_2\text{-}PPh_2)_2]^-$ forms monoclinic crystals with unit-cell dimensions a = 10.227 (4) Å, b = 18.189 (6) Å, c = 12.788 (5) Å, β = 91.07 (3)°, and symmetry $P2_1$; d_{calcd} = 1.33 g/cm^3 for Z = 2 vs. d_{obsd} = 1.33 g/cm^3. Least-squares refinement converged at $R_1(F)$ = 5.1% and $R_2(F)$ = 5.6% for 2418 reflections with $F_o^2 > 3\sigma(F_o^2)$.

Introduction

Recent work by Collman et al.[2] has shown that the reduced phosphido-bridged iron dimer, the $[Fe_2(CO)_6(\mu_2\text{-}PPh_2)_2]^{2-}$ dianion, can be used to produce aldehydes in quantitative yield by reaction with alkyl halides and tosylates followed by protonation of the acyl products. This discovery not only prompted an investigation by them of the mechanism of this reaction including a spectroscopic examination of the nature of the intermediates[2] but also led to the successful structural determination[3] by X-ray diffraction of the highly unusual geometry of the important (metal-metal)-nonbonding $[Fe_2(CO)_6(\mu_2\text{-}PPh_2)_2]^{2-}$ dianion.

The formation of a red, crystalline acyl complex, $Na[Fe_2(CO)_5(C(O)R)(\mu_2\text{-}PPh_2)_2]\cdot 2THF$, was attributed by Collman and co-workers[2] to an oxidative addition of RX to the dianion in THF, thereby affording an iron–alkyl intermediate (not detected) which rapidly rearranged to the above binuclear iron acyl complex via alkyl migration. Two extreme hypothetical structures (I and II) were initially proposed for these acyl monoanions in accord with the conformity of the metal atoms to the EAN rule. Structure I has an acyl ligand which bridges both metal atoms (with no metal–metal bond then being required), while structure II has no coordination of the acyl oxygen atom to the second metal atom (which then necessitates a metal–metal bond). Precedence for such two-atom bridged acyl ligands had been established from structural studies[4,5] of two unusual types of binuclear transition metal acyl complexes, III and IV (for each of which the metal atoms comply with the EAN rule). One type, III, containing an electron-pair Fe–Fe bond (2.568 (2) Å), was determined by

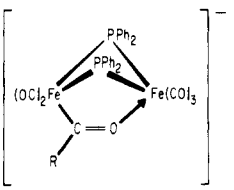

I

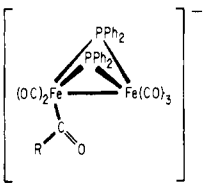

II

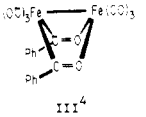

III[4]

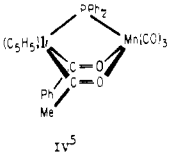

IV[5]

0002-7863/79/1501-7218$01.00/0

Lindley and Mills[4] to have the carbon atoms of both benzoyl (alternatively denoted[4] as phenyloxycarbene) ligands unexpectedly coordinated to the same Fe atom; the iridium–manganese complex, IV, was found by Kaesz and co-workers[5] to contain iridium-coordinated acetyl and benzoyl ligands with each bonded through its oxygen atom to the Mn atom, which is nonbonding with the iridium atom (with Ir···Mn 3.543 (2) Å).

Herein we report the structures of the first examples of binuclear metal acyl complexes with no coordination of the acyl oxygen atom to the second metal atom (viz., of type II with an Fe–Fe bond). Both the $[Na(THF)_2]^+$ and $[(Ph_3P)_2N]^+$ salts of the acetyl monoanion (R = CH_3) were chosen for a crystallographic examination not only to differentiate between the two possible models I and II but also to determine any pronounced effect of the alkali metal ion on the geometry of the monoanion due to presumed ion pairing of the sodium ion in contrast to none being assumed for the bis(triphenylphosphine)iminium cation. While this structural investigation was in progress, Rothrock and Collman[6] found that the addition of phenyllithium to $Fe_2(CO)_6(\mu_2\text{-}PPh_2)_2$ in THF yielded the corresponding lithium benzoyl complex—viz., $[Li(THF)_3]^+[Fe_2(CO)_5(C(O)Ph)(\mu_2\text{-}PPh_2)_2]^-$. Its X-ray analysis (by J.M.B. and K.O.H.) has provided particularly important stereochemical information, which, in conjunction with that obtained (by R.E.G. and L.F.D.) for the $[Na(THF)_2]^+$ and $[(Ph_3N)_2N]^+$ salts, has enabled a detailed assessment of the type and extent of ion pairing of alkali metal cations with metal acyl carbonylate anions in the solid state.

This work is of special relevance with respect to the determined role of ion pairing reported by Collman, Cawse, and Brauman[7] in 1972 for the reactions of alkyl $[Fe(CO)_4R]^-$ monoanions with L ligands such as tertiary phosphines to give acyl $[Fe(CO)_3L(C(O)R)]^-$ monoanions. From their observation that the effect of the cation on the rates of alkyl–acyl migratory insertions in THF was remarkably dependent on the nature of the cation with $Li^+ > Na^+ \gg [(Ph_3P)_2N]^+$, they found that the results are consistent with a mechanism in which a sodium or lithium ion pair is the kinetically reactive species. They concluded that formation of the acyl monoanion is facilitated by electrostatic interaction of small polarizing cations which help stabilize the extra negative charge developed on the acyl oxygen atom. They also pointed out that ion-paired structures for alkali metal salts of metal carbonyl anions, whose existence was first recognized by Edgell and co-workers[8] from their extensive IR studies of $NaCo(CO)_4$ in THF, may have hitherto unrecognized consequences in the chemical reactivity of many metal carbonyl anions. Other subsequent solution studies[9,10] have probed the nature and importance of ion pairing of alkali metal cations with various metal carbonylate anions. Of particular interest are the solvent effects on the solution structure proposed by Darensbourg and Burns[9b] for the lithium salt of the acyl $[trans\text{-}(Ph_3P)Fe(CO)_3(C(O)Ph)]^-$ monoanion as inferred from their IR investigation as a function of solvent. Direct evidence was presented[9b] for a tight lithium ion pairing with a carbonyl oxygen atom as well as with the acyl oxygen atom in diethyl ether, whereas the (carbonyl oxygen)–Li^+ ion pair is separated by the addition of small quantities of either tetrahydrofuran or *N,N*-dimethylformamide.

Besides providing definitive evidence for the occurrence of tight ion interactions of alkali metal ions with carbonyl oxygen atoms as well as with the acyl oxygen atoms in metal acyl carbonylate anions, the crystallographic work presented here supplements the recent X-ray diffraction studies by Bau and co-workers[11] of $Na_2[Fe(CO)_4]\cdot 1.5(C_4H_8O_2)$,[11a] $K_2[Fe(CO)_4]$,[11b] and $[Na(2,2,2\text{-crypt})]_2[Fe(CO)_4]$,[11b] which showed a dramatic dependence of the $[Fe(CO)_4]^{2-}$ geometry on the counterion. In marked contrast to an essentially regular tetrahedral configuration being found for the $[Fe(CO)_4]^{2-}$ dianion in the $[Na(2,2,2\text{-crypt})]^+$ salt (in which the Na^+ ion is completely encapsulated by the cryptand chelator), a highly distorted configuration was observed in the sodium salt, and a less distorted configuration in the potassium salt.[11] Of obvious interest was to discern whether this large geometrical dependence of a metal carbonylate anion on the decreasing polarizing capacity of the Na^+, K^+, and $[Na(2,2,2\text{-crypt})]^+$ ions was also observed for a metal acyl carbonylate anion due to the widely differing nature of the Li^+, Na^+, and $[(Ph_3P)_2N]^+$ counterions.

Experimental Section

General Remarks. Details of the syntheses and spectroscopic characterization of the three compounds reported here are given elsewhere.[2,6] All reactions were carried out with rigorous exclusion of O_2 and water by use of a nitrogen-filled drybox. Crystals of $[Na(THF)_2]^+[Fe_2(CO)_5(C(O)Me)(\mu_2\text{-}PPh_2)_2]^-$ were obtained from a THF solution to which a dropwise addition of hexane initiated crystallization. The corresponding $[(Ph_3P)_2N]^+$ salt was prepared by the addition of an excess of $[(Ph_3P)_2N]^+Cl^-$ in acetone solution to an acetone solution of the $[Na(THF)_2]^+$ salt followed by filtration. A 1/1 mixture (v/v) of diethyl ether/hexane was added to the filtrate which, after being cooled to −22 °C, produced red-orange crystals of $[(Ph_3P)_2N]^+[Fe_2(CO)_5(C(O)Me)(\mu_2\text{-}PPh_2)_2]^-$. Crystals of $[Li(THF)_3]^+[Fe_2(CO)_5(C(O)Ph)(\mu_2\text{-}PPh_2)_2]^-$ were likewise obtained from a THF solution to which hexane was added to initiate crystallization.

Crystal Data and X-ray Data Collection. A. The $[(Ph_3P)_2N]^+$ and $[Na(THF)_2]^+$ Salts of the $[Fe_2(CO)_5(C(O)Me)(\mu_2\text{-}PPh_2)_2]^-$ Monoanion. Suitable crystals selected from an optical examination were mounted under argon inside thin-walled Lindemann glass capillaries. The particular crystal of the $[(Ph_3P)_2N]^+$ salt utilized for the X-ray diffraction study was an orthorhombic-shaped plate with dimensions 0.50 × 0.10 × 0.36 mm. Problems were encountered in attempted X-ray measurements of several mounted crystals of the $[Na(THF)_2]^+$ salt owing to rapid decay of the crystals after several hours of X-ray beam exposure, during which time the translucent red-orange crystals turned opaque. After unsuccessful efforts for crystals wedged inside the sealed capillaries under argon, a crystal was mounted under argon in a thin-walled capillary and then completely coated with quick-drying epoxy cement. Data collection was successfully achieved for this crystal without decay problems. The dimensions for this orthorhombic-shaped crystal were 0.60 × 0.20 × 0.20 mm.

Intensity data were collected on a Syntex $P\bar{1}$ diffractometer equipped with a scintillation counter, a pulse-height analyzer adjusted to admit 90% of the Mo $K\bar{\alpha}$ radiation, and a crystal graphite monochromator set at a Bragg 2θ angle of 12.2°. For each compound 15 reflections obtained from a rotation photograph were centered automatically and used in a least-squares refinement to determine the crystal system (whose symmetry and lattice lengths were confirmed from axial photographs), lattice constants, and the orientation matrix, from which the angle settings for all reflections were calculated. In the case of the $[(Ph_3P)_2N]^+$ salt, more precise lattice constants and the orientation matrix were obtained by a fast sampling of data between 20 and 25° in 2θ, with only those reflections with diffraction maxima greater than 150 counts being recorded. Fifteen reflections so identified were subsequently used in a redetermination of the lattice constants and orientation matrix. This procedure was not followed with the $[Na(THF)_2]^+$ salt owing to concern about crystal decay. Lattice constants determined at the ambient temperature of 22 °C for the orthorhombic unit cell of $[(Ph_3P)_2N]^+[Fe_2(CO)_5(C(O)Me)(\mu_2\text{-}PPh_2)]^-$ (formula wt 1189 g/mol) are a = 14.725 (4), b = 11.608 (6), and c = 17.387 (5) Å. The cell volume of 2972 Å^3 gives a calculated density of 1.32 g/cm^3 for Z = 2. Lattice constants obtained at 22 °C for the monoclinic unit cell of $[Na(C_4H_8O)_2]^+[Fe_2(CO)_5(C(O)Me)(\mu_2\text{-}PPh_2)]^-$ (formula wt 832 g/mol) are a = 9.284 (7) Å, b = 23.889 (21) Å, c = 18.427 (14) Å, and β = 99.45 (6)°. The cell volume of 4031 Å^3 results in d_{calcd} = 1.37 g/cm^3 for Z = 4.

In both cases intensity data were acquired by the θ–2θ scan technique with (stationary crystal)–(stationary counter) background counting at both extremes of each scan and with a variable scan speed of from 2.00 to 24.00°/min in 2θ. The ratio of total background time to scan time was 0.67, and the scan speeds and widths for individual diffraction maxima were determined by relative peak intensities. Two standard reflections, which were measured after every 48 data re-

flections, showed no significant changes in their intensities during the entire data collection. Data were sampled once in the independent orthorhombic octant hkl for $3.0° \leq 2\theta \leq 40.0°$ for the $[(Ph_3P)_2N]^+$ salt, and once in the independent monoclinic octants hkl and $h\bar{k}l$ for $3.0° \leq 2\theta \leq 50.0°$ for the $[Na(THF)_2]^+$ salt.

The measured intensities of 1627 and 7517 reflections for the $[(Ph_3P)_2N]^+$ and $[Na(THF)_2]^+$ salts, respectively, were corrected[12a] for background and polarization of the incident beam due to the crystal monochromator and then were merged[12b] to yield 1516 and 6888 independent data for the $[(Ph_3P)_2N]^+$ and $[Na(THF)_2]^+$ salts, respectively, of which 1213 reflections for the $[(Ph_3P)_2N]^+$ salt and 1708 reflections for the $[Na(THF)_2]^+$ salt with $I \geq 2\sigma(I)$ were utilized in the structural refinements.

Absorption corrections[12c] were applied to the intensity data of both compounds in that the transmission coefficients (for Mo K$\bar{\alpha}$ radiation) varied from 0.73 to 0.94 in the $[(Ph_3P)_2N]^+$ salt (for which the calculated linear absorption coefficient, μ, was 6.56 cm^{-1})[13] and from 0.75 to 0.85 in the $[Na(THF)_2]^+$ salt (for which μ was 8.79 cm^{-1}).[13]

B. The $[Li(THF)_3]^+$ Salt of the $[Fe_2(CO)_5(C(O)Ph)(\mu_2\text{-}PPh_2)_2]^-$ Monoanion. A suitable crystal of dimensions 0.30 × 0.35 × 0.30 mm was mounted and sealed in a glass capillary under a nitrogen atmosphere. This capillary was mounted on a goniometer head and placed on a Syntex $P2_1$ diffractometer. Thirteen reflections, identified from a rotation photograph, were automatically centered. The monoclinic cell was selected from the diffractometer-generated axis solutions consistent with these 13 reflections. Partial rotation photographs were taken around all three axes to confirm the Laue C_{2h}-$2/m$ diffraction symmetry. The final lattice constants and orientation matrix were determined by least-squares refinement of the 13 reflections ($3° < 2\theta < 11°$). The crystal gave ω-scan widths at half-height of ca. 0.18° for five low-angle reflections. The determined lattice constants at room temperature for $[Li(THF)_3]^+[Fe_2(CO)_5(C(O)Ph)(\mu_2\text{-}PPh_2)_2]^-$ (formula wt 951 g/mol) are a = 10.227 (4) Å, b = 18.189 (6) Å, c = 12.788 (5) Å, and β = 91.07 (3)° with V = 2378 Å^3; the calculated density of 1.33 g/cm^3 for $Z = 2$ is identical with the observed value determined by the flotation method in hexane and CCl_4.

Intensity data were acquired in the θ-2θ scan mode with graphite monochromated Mo K$\bar{\alpha}$ radiation, in which the takeoff angle for the X-ray tube was 3° and the Bragg 2θ angle for the monochromator was 12.2°. The data were collected with a scan width of 1.2° and a variable scan rate ranging from 2.0 to 29.3°/min. Stationary-background counts were taken at the beginning and end of each scan with a (total background time) to (scan time) ratio of 0.25. Three standard reflections (011, 020, and 110) were monitored every 50 reflections as a check for crystal and instrumental stability; no systematic fluctuation or decrease of the standard intensities was observed during the entire data collection.

One-fourth of the full sphere of data ($+h$, $+k$, $\pm l$) was collected with $2\theta(\text{max}) = 40°$ giving a total of 4625 reflections. The data processing was performed by the program ENXDR.[14] The parameter p, introduced to avoid overweighting the strong reflections, was set to 0.05. The corrected intensities were converted to values for F_o^2 by application of Lorentz and polarization corrections. An absorption correction was applied by use of a Gaussian numerical integration program.[14] The applied corrections (based on $\mu = 7.49$ cm^{-1} for Mo K$\bar{\alpha}$ radiation)[13] on F_o^2 ranged from 1.14 to 1.22 with an average correction of 1.20. There were 2418 reflections with $F_o^2 > 3\sigma(F_o^2)$ used in the final refinement.

Structural Determination and Refinement. A. $[(Ph_3P)_2N]^+[Fe_2(CO)_5(C(O)Me)(\mu_2\text{-}PPh_2)_2]^-$. Systematic absences of $\{h00\}$ for h odd and $\{00l\}$ for l odd uniquely suggested the probable orthorhombic space group to be $P2_12_12_1$ (nonstandard setting of $P2_12_12(D_2^3$, no. 18)[15a] for $a\ \bar{c}\ b$)[16a] such that the crystallographically independent unit consists of one-half of the acyl monoanion and one-half of the $[(Ph_3P)_2N]^+$ cation (each of which is required to possess crystallographic C_2-2 site symmetry). An analysis of a three-dimensional Patterson map by PHASE[12d] revealed the position of the independent Fe atom, after which the remaining nonhydrogen atoms (except the acyl atoms) were located by successive Fourier syntheses.[12e,17,18a,b] At this point it was realized that there was a crystallographic twofold disorder of the monoanion effectively involving the acyl atoms and one of the two equatorial carbonyl ligands on the other Fe atom being nearly superimposed. The crystallographic twofold axis passing through the center of the bent Fe_2P_2 core results in their random distribution between two half-weighted orientations. Therefore, least-squares refinement[12f,19,20] was performed on the nondisordered fragment with a full-weighted carbonyl ligand (included as a fixed contribution to the structure factor calculations) situated at the mean location of the half-weighted crystal-disordered acyl and carbonyl positions. After several cycles of least-squares refinement of the other nonhydrogen atoms, the fixed carbonyl group was removed and the positions of the disordered acyl and carbonyl ligands were then located from a difference Fourier map. Isotropic least squares of all nonhydrogen atoms, with the crystal disordered atoms included with half-weighted occupancy, converged at $R_1(F)$ = 9.23% and $R_2(F)$ = 10.09%. Further least-squares refinement with anisotropic temperature factors utilized for the nondisordered atoms of the acyl monoanion and for the phosphorus and nitrogen atoms of the $[(Ph_3P)_2N]^+$ cation gave $R_1(F)$ = 7.53% and $R_2(F)$ = 8.19%. At this point idealized positions were calculated[12g] for the hydrogen atoms. Full-matrix least-squares refinement[12h] of all nonhydrogen parameters (with fixed hydrogen contributions to the structure factors[17,18b]) lowered $R_1(F)$ to 6.9% and $R_2(F)$ to 7.6%.

The absolute configuration of the crystal structure was then determined from the effects of anomalous dispersion.[17,18c,d] Least-squares refinements of both configurations (with the second one obtained by a relabeling of the hkl indices as $\bar{h}\bar{k}\bar{l}$) were performed with fixed hydrogen contributions until convergence (i.e., until Δ/σ values were less than 0.05); the discrepancy factors of $R_1(F)$ = 6.80% and $R_2(F)$ = 7.45% for the hkl indices were found to be slightly higher than those of $R_1(F)$ = 6.55% and $R_2(F)$ = 7.15% for the $\bar{h}\bar{k}\bar{l}$ indices. Hence, the structure as refined for the $\bar{h}\bar{k}\bar{l}$ indices is reported here. A final three-dimensional Fourier difference map showed no unusual features with only one peak of 1.3 e$^-$/Å^3 greater than 1.0 e$^-$/Å^3; no physically reasonable atom could be assigned to this peak.

The atomic parameters from the output of the final cycle of the full-matrix least-squares refinement are given in Table I. Interatomic distances and bond angles with estimated standard deviations[12i] are listed in Table II. Selected least-squares planes[12j] and interplanar angles are presented in Table III. Observed and calculated structure factors are given as supplementary material.

B. $[Na(THF)_2]^+[Fe_2(CO)_5(C(O)Me)(\mu_2\text{-}PPh_2)_2]^-$. Systematic absences of $h + l$ odd for $\{h0l\}$ and k odd for $\{0k0\}$ uniquely indicated the probable monoclinic space group to be $P2_1/n$(C_{2h}^5, no. 14).[16b] The crystallographically independent unit consists of one complete dimeric acyl monoanion and one $[Na(THF)_2]^+$ monocation. An interpretation of a computed three-dimensional Patterson synthesis provided initial positions for the two independent iron atoms; successive Fourier and difference Fourier syntheses eventually yielded coordinates for all nonhydrogen atoms of the monoanion, the sodium ion, and the two (C_4H_8O) solvent molecules. The presence of these two THF molecules in the crystalline state was in agreement with their prior determination by elemental analysis and by NMR measurements on crystalline material.[2,6] Initial least squares with isotropic temperature factors yielded $R_1(F)$ = 14.56% and $R_2(F)$ = 13.7%. Considerable difficulty was experienced with one of the two THF solvent molecules. At this stage of refinement one THF molecule was reasonably well behaved, but the atoms of the other THF molecule had poorly defined coordinates and unusually large isotropic temperature factors. Subsequent difference Fourier syntheses indicated that this THF molecule was disordered between two crystal orientations. Inclusion of the second THF molecule (with both orientations half-weighted) did not significantly improve the refinement. Further refinement[12h] was attempted with anisotropic thermal parameters for various nonhydrogen atoms, but these different thermal models did not significantly lower the $R_1(F)$ and $R_2(F)$ values. Attempts to model the crystal disorder with a rigid-group constraint[12h] of the THF molecule to an idealized geometry followed by an anisotropic thermal refinement with fixed x, y, z coordinates also did not provide a better resolution of the problem. However, it was encouraging to note that the positional parameters of all other atoms including those of the well-defined THF molecule were essentially invariant to the different models utilized for the nonhydrogen atoms of the ill-defined THF molecule. In light of this, the final refinement[12h] used an anisotropic thermal model for the iron, phosphorus, and sodium atoms and an isotropic thermal model for the other nonhydrogen atoms. Idealized coordinates[12g] and isotropic temperature factors for the hydrogen atoms on the acyl methyl carbon atom and on the phenyl carbon atoms were included as fixed contributors[17,18b] in the final cycles. This last refinement[12h] converged at $R_1(F)$ = 12.9% and $R_2(F)$ = 11.4% with a "goodness-of-fit" value of 1.54 and with the largest shift-over-error

Table I. Atomic Parameters[a] for $[(Ph_3P)_2N]^+[Fe_2(CO)_5(C(O)Me)(\mu_2\text{-}PPh_2)_2]^-$

	x	y	z	B, Å^2		x	y	z	B, Å^2
Fe	−0.4180(2)	−0.9274(2)	−0.0358(1)	*b*	CD(6)	−0.0841(12)	−1.6634(16)	0.0725(10)	5.56
P(1)	−0.5446(3)	−0.8391(4)	−0.0733(2)	*b*	CE(1)	0.1130(10)	−1.4135(14)	0.1263(8)	3.24
PP	0.0065(3)	−1.4569(4)	0.0875(2)	*b*	CE(2)	0.1844(12)	−1.3887(15)	0.0710(10)	4.80
N	0.0000(−)	−1.4299(16)	0.0000(−)	*b*	CE(3)	0.2686(13)	−1.3476(17)	0.1005(12)	6.50
O(1)	−0.4282(10)	−1.0936(12)	−0.1606(6)	*b*	CE(4)	0.2824(11)	−1.3318(15)	0.1744(10)	4.27
C(1)	−0.4271(13)	−1.0265(14)	−0.1136(10)	*b*	CE(5)	0.2141(11)	−1.3576(15)	0.2272(10)	4.28
O(2)	−0.2635(10)	−0.7922(14)	−0.0791(9)	*b*	CE(6)	0.1316(11)	−1.3966(15)	0.2036(9)	4.20
C(2)	−0.3283(12)	−0.8471(20)	−0.0611(11)	*b*	H(1-1)[c]	−0.319	−1.201	0.032	6.0
C(2-1)	−0.3531(26)	−1.1317(33)	0.0490(22)	2.82	H(2-1)	−0.412	−1.148	0.051	6.0
C(1-1)	−0.3334(23)	−1.0388(27)	0.0091(18)	3.11	H(3-1)	−0.336	−1.120	0.100	6.0
O(1-1)	−0.2481(17)	−1.0377(20)	0.0072(14)	5.86	HA(2)	−0.416	−0.651	−0.105	6.0
O(3)	−0.3883(21)	−1.1439(25)	0.0557(16)	2.40	HA(3)	−0.450	−0.427	−0.121	6.0
C(3)	−0.3941(25)	−1.0500(32)	0.0259(20)	4.29	HA(4)	−0.597	−0.354	−0.111	6.0
CA(1)	−0.5567(10)	−0.6821(12)	−0.0832(8)	2.82	HA(5)	−0.724	−0.480	−0.080	6.0
CA(2)	−0.4829(11)	−0.6129(14)	−0.0988(10)	4.33	HA(6)	−0.699	−0.689	−0.055	6.0
CA(3)	−0.5041(16)	−0.4879(17)	−0.1094(11)	6.65	HB(2)	−0.475	−0.842	−0.234	6.0
CA(4)	−0.5867(14)	−0.4453(18)	−0.1018(11)	6.50	HB(3)	−0.545	−0.893	−0.358	6.0
CA(5)	−0.6567(13)	−0.5152(17)	−0.0852(11)	5.62	HB(4)	−0.698	−0.962	−0.365	6.0
CA(6)	−0.6428(11)	−0.6352(15)	−0.0725(10)	4.06	HB(5)	−0.791	−0.982	−0.250	6.0
CB(1)	−0.5962(10)	−0.8805(12)	−0.1655(8)	2.88	HB(6)	−0.725	−0.924	−0.118	6.0
CB(2)	−0.5452(10)	−0.8718(13)	−0.2349(9)	3.56	HC(2)	−0.099	−1.508	0.226	6.0
CB(3)	−0.5847(12)	−0.9025(14)	−0.3062(9)	4.80	HC(3)	−0.214	−1.386	0.296	6.0
CB(4)	−0.6698(13)	−0.9394(18)	−0.3104(10)	5.68	HC(4)	−0.264	−1.210	0.252	6.0
CB(5)	−0.7221(11)	−0.9485(16)	−0.2461(10)	4.87	HC(5)	−0.194	−1.128	0.129	6.0
CB(6)	−0.6843(10)	−0.9178(14)	−0.1696(8)	3.53	HC(6)	−0.076	−1.232	0.061	6.0
CC(1)	−0.0824(11)	−1.3770(16)	0.1393(9)	3.25	HD(2)	0.102	−1.625	0.187	6.0
CC(2)	−0.1199(12)	−1.4229(17)	0.2073(10)	5.10	HD(3)	0.067	−1.847	0.203	6.0
CC(3)	−0.1838(11)	−1.3559(16)	0.2426(9)	4.32	HD(4)	−0.070	−1.924	0.153	6.0
CC(4)	−0.2123(12)	−1.2556(17)	0.2197(11)	5.50	HD(5)	−0.150	−1.827	0.051	6.0
CC(5)	−0.1730(13)	−1.2093(16)	0.1516(11)	5.70	HD(6)	−0.129	−1.614	0.036	6.0
CC(6)	−0.1069(12)	−1.2695(16)	0.1124(10)	5.41	HE(2)	0.173	−1.405	0.010	6.0
CD(1)	−0.0116(12)	−1.6067(14)	0.1098(9)	4.24	HE(3)	0.322	−1.321	0.062	6.0
CD(2)	0.0460(13)	−1.6675(18)	0.1584(12)	6.77	HE(4)	0.348	−1.304	0.194	6.0
CD(3)	0.0245(16)	−1.7908(20)	0.1696(13)	8.21	HE(5)	0.225	−1.346	0.288	6.0
CD(4)	−0.0485(16)	−1.8370(21)	0.1384(14)	8.40	HE(6)	0.078	−1.414	0.244	6.0
CD(5)	−0.1007(13)	−1.7818(18)	0.0840(12)	6.79					

	β_{11}	β_{22}	β_{33}	β_{12}	β_{13}	β_{23}		β_{11}	β_{22}	β_{33}	β_{12}	β_{13}	β_{23}
Fe	55	73	23	16	−8	−8	O(1)	102	153	34	30	−4	−47
P(1)	54	67	19	11	−3	−3	C(1)	67	52	40	13	−15	8
PP	54	67	26	14	1	5	O(2)	71	194	70	3	17	−8
N	93	48	25	0	−6	0	C(2)	36	163	36	9	−8	−44

[a] Estimated standard deviations of least significant figures are given in parentheses. [b] Anisotropic thermal parameters of the form $\exp[-(\beta_{11}h^2 + \beta_{22}k^2 + \beta_{33}l^2 + 2\beta_{12}hk + 2\beta_{13}hl + 2\beta_{23}kl)]$ were used. The resulting thermal coefficients, β_{ij} ($\times 10^4$), are listed. [c] During least-squares refinement, the positional parameters of the hydrogen atoms and their arbitrarily assigned isotropic temperature factors of 6.0 Å^2 were held constant.

ratio (Δ/σ) of 0.25%. A final difference Fourier map showed a maximum residual electron density of 1.4 e$^-$/Å^3; the ten residual peaks down to 0.7 e$^-$/Å^3, which were associated with the nonhydrogen atoms of the monoanion and not with the solvent molecules, were found to be physically nonmeaningful.

The positional and thermal parameters from the output of the final cycle of the least-squares refinement are given in Table IV. Interatomic distances and bond angles with estimated standard deviations[12i] are given in Table V. Table VI gives selected least-squares planes[12j] with interplanar angles. A listing of the observed and calculated structure factors is available as supplementary material.

C. $[Li(THF)_3]^+[Fe_2(CO)_5(C(O)Ph)(\mu_2\text{-}PPh_2)_2]^-$. An examination of the intensity data revealed only $\{0k0\}$ absent for k odd, thus indicating that the probable monoclinic space group was either $P2_1$ (C_2^2, no. 4)[15b] or $P2_1/m$ (C_{2h}^2, no. 11).[15c] Wilson statistics, calculated by the program FAME,[14] and the Howells-Philips-Rogers zero-moment test[21] both indicated noncentric intensity distributions. Thus, the space group was tentatively chosen as $P2_1$. The subsequent structural determination and successful refinement substantiated this choice.

Initial positions for the two independent Fe atoms were found from a three-dimensional Patterson map. The origin was established by the fixing of the y coordinate of one of the Fe atoms at 0.25. Three cycles of isotropic least-squares refinement[17,18a,19,20] followed by calculation of a difference Fourier map led to the location of the two P atoms. Several cycles of least squares followed by difference Fourier syntheses revealed all of the remaining nonhydrogen atoms. On the basis of their large (12-18 Å^2) isotropic thermal parameters, the three THF molecules seemed to be somewhat disordered. In one of the THF molecules this disorder was clearly more severe, as the thermal parameters for the carbon atoms (as originally located) would refine only to unreasonably high values. A difference Fourier map calculated with the four THF carbon atoms excluded revealed six large peaks in the vicinity of the THF molecule, thus indicating the presence of two distinct orientations for two of the ring carbon atoms. The use of these two pairs of half-occupied positions resulted in refined isotropic thermal parameters comparable to those for the carbon atoms in the other THF molecules. The structure was then refined anisotropically except for the two disordered carbon atoms for which an isotropic thermal model was still utilized. Idealized hydrogen positions for the five phenyl rings were calculated from an assumed standard geometry with C-H distances of 1.0 Å. The hydrogen coordinates were not refined but were included as fixed contributions[18b] in the last three cycles of least-squares refinement. The discrepancy factors at convergence for the configuration determined by anomalous dispersion effects[18d] were $R_1(F) = 5.1\%$ and $R_2(F) = 5.6\%$. The "goodness-of-fit" value was 1.32. A final difference Fourier synthesis showed no peaks greater than

Table II. Interatomic Distances and Bond Angles for $[(Ph_3P)_2N]^+[Fe_2(CO)_5(C(O)Me)(\mu_2\text{-}PPh_2)_2]^-$ [a]

A. Intraanion Distances (Å)

Fe-Fe′	2.718(5)	Fe′···C(2-1)	4.11(4)
Fe-P	2.225(5)	P-CB(1)	1.84(1)
Fe-P′	2.226(5)	CB(1)-CB(2)	1.42(2)
P···P′	2.867(9)	CB(2)-CB(3)	1.42(2)
Fe-C(1)	1.78(2)	CB(3)-CB(4)	1.33(2)
Fe-C(2)	1.67(2)	CB(4)-CB(5)	1.36(2)
Fe-C(3)	1.82(4)	CB(5)-CB(6)	1.49(2)
C(1)-O(1)	1.13(2)	CB(6)-CB(1)	1.37(2)
C(2)-O(2)	1.19(2)	P-CA(1)	1.84(1)
C(3)-O(3)	1.21(4)	CA(1)-CA(2)	1.38(2)
Fe-C(1-1)	1.96(3)	CA(2)-CA(3)	1.49(2)
C(1-1)-O(1-1)	1.26(3)	CA(3)-CA(4)	1.32(2)
C(1-1)-C(2-1)	1.31(4)	CA(4)-CA(5)	1.34(2)
O(1-1)···C(2-1)	2.03(5)	CA(5)-CA(6)	1.42(2)
Fe···O(1-1)	2.91(2)	CA(6)-CA(1)	1.39(2)
Fe···C(2-1)	2.95(4)		

B. Intracation Distances (Å)

PP-N	1.556(6)	CD(5)-CD(6)	1.41(2)
PP···PP″	3.049(9)	CD(6)-CD(1)	1.41(2)
PP-CC(1)	1.84(2)	PP-CE(1)	1.78(1)
CC(1)-CC(2)	1.41(2)	CE(1)-CE(2)	1.45(2)
CC(2)-CC(3)	1.37(2)	CE(2)-CE(3)	1.42(2)
CC(3)-CC(4)	1.30(2)	CE(3)-CE(4)	1.31(2)
CC(4)-CC(5)	1.42(2)	CE(4)-CE(5)	1.39(2)
CC(5)-CC(6)	1.38(2)	CE(5)-CE(6)	1.36(2)
CC(6)-CC(1)	1.38(2)	CE(6)-CE(1)	1.38(2)
PP-CD(1)	1.80(2)	N···CC(1)	2.79(2)
CD(1)-CD(2)	1.39(2)	N···CD(1)	2.81(2)
CD(2)-CD(3)	1.48(3)	N···CE(1)	2.76(1)
CD(3)-CD(4)	1.32(3)	CC(1)···CD(1)	2.91(2)
CD(4)-CD(5)	1.38(3)	CC(1)···CE(1)	2.92(2)
		CD(1)···CE(1)	2.91(2)

C. Intraanion Bond Angles (deg)

Fe-P-Fe′	75.3(2)	P-CA(1)-CA(6)	117.5(12)
P-Fe-P′	80.2(2)	CA(1)-CA(2)-CA(3)	115.2(16)
P-Fe-C(1)	90.7(6)	CA(2)-CA(3)-CA(4)	123.0(19)
P-Fe-C(2)	109.1(7)	CA(3)-CA(4)-CA(5)	120.1(19)
P-Fe-C(3)	134.1(12)	CA(4)-CA(5)-CA(6)	120.9(19)
P-Fe-C(1-1)	162.5(10)	CA(5)-CA(6)-CA(1)	119.5(17)
P′-Fe-C(1)	157.8(6)	CA(6)-CA(1)-CA(2)	121.1(14)
P′-Fe-C(2)	99.3(6)	P-CB(1)-CB(2)	120.1(11)
P′-Fe-C(3)	84.5(11)	P-CB(1)-CB(6)	121.3(12)
P′-Fe-C(1-1)	96.9(9)	CB(1)-CB(2)-CB(3)	120.5(14)
C(1)-Fe-C(2)	102.7(10)	CB(2)-CB(3)-CB(4)	121.2(17)
C(1)-Fe-C(3)	87.6(12)	CB(3)-CB(4)-CB(5)	121.0(18)
C(1)-Fe-C(1-1)	85.7(11)	CB(4)-CB(5)-CB(6)	120.3(16)
C(2)-Fe-C(3)	116.0(13)	CB(5)-CB(6)-CB(1)	118.5(14)
C(2)-Fe-C(1-1)	88.3(12)	CB(6)-CB(1)-CB(2)	118.6(14)
Fe-C(1-1)-O(1-1)	128.2(26)	P-CA(1)-CA(2)	121.3(11)
Fe-C(1-1)-C(2-1)	127.8(29)		
C(2-1)-C(1-1)-O(1-1)	104.0(32)		
Fe-C(1)-O(1)	175.2(16)		
Fe-C(2)-O(2)	178.5(20)		
Fe-C(3)-O(3)	166.4(30)		
Fe-P-CA(1)	124.4(5)		
Fe-P-CB(1)	118.8(5)		
Fe′-P-CA(1)	120.8(5)		
Fe′-P-CB(1)	121.4(5)		

D. Intracation Angles (deg)

PP-N-PP″	156.7(15)	PP-CD(1)-CD(2)	122.1(14)
		PP-CD(1)-CD(6)	117.6(14)
N-PP-CC(1)	109.5(7)		
N-PP-CD(1)	113.3(9)	CD(1)-CD(2)-CD(3)	116.2(20)
N-PP-CE(1)	111.6(6)	CD(2)-CD(3)-CD(4)	120.9(24)
		CD(3)-CD(4)-CD(5)	123.3(25)
CC(1)-PP-CD(1)	106.0(7)	CD(4)-CD(5)-CD(6)	117.0(21)
CC(1)-PP-CE(1)	107.3(7)	CD(5)-CD(6)-CD(1)	121.3(18)
CD(1)-PP-CE(1)	108.8(8)	CD(6)-CD(1)-CD(2)	120.3(16)
PP-CC(1)-CC(2)	120.0(13)	PP-CE(1)-CE(2)	116.2(11)
PP-CC(1)-CC(6)	118.4(13)	PP-CE(1)-CE(6)	125.7(12)
CC(1)-CC(2)-CC(3)	115.6(17)	CE(1)-CE(2)-CE(3)	117.2(16)
CC(2)-CC(3)-CC(4)	126.4(18)	CE(2)-CE(3)-CE(4)	122.3(19)
CC(3)-CC(4)-CC(5)	117.6(19)	CE(3)-CE(4)-CE(5)	120.2(18)
CC(4)-CC(5)-CC(6)	120.5(18)	CE(4)-CE(5)-CE(6)	121.1(16)
CC(5)-CC(6)-CC(1)	118.4(17)	CE(5)-CE(6)-CE(1)	121.2(16)
CC(6)-CC(1)-CC(2)	121.5(16)	CE(6)-CE(1)-CE(2)	118.0(14)

E. Selected Interatomic Distances and Angles for Those Atoms Involved in Hydrogen Bonding with the Acyl Ligand in $[Ph_3PNPPh_3]^+[Fe_2(CO)_5(C(O)Me)(\mu_2\text{-}PPh_2)_2]^-$

O(1-1)···CC(5)	3.39(3)	CB(6)-HB(6)-O(1-1)	144(1)
O(1-1)···HC(5)	2.49	CC(5)-HC(5)-O(1-1)	141(1)
O(1-1)···CB(6)	3.30(4)		
O(1-1)···HB(6)	2.37		

[a] All atoms with primes refer to the symmetry-related position $-1-x, y, -z$, while all atoms with double primes refer to the symmetry-related position $-x, y, -z$.

30% of the height of a carbon atom peak, and, in particular, no abnormally large peaks around the THF molecules.

The atomic coordinates from the output of the last cycle are listed in Table VII, while interatomic distances and bond angles are presented in Table VIII. Least-squares planes[13] along with interplanar angles are found in Table IX. Observed and calculated structure factors are available as supplementary material.

Results and Discussion

Description of the Structures of the Acyl Complexes. The basic structures of the $[Fe_2(CO)_5(C(O)R)(\mu_2\text{-}PPh_2)]^-$ monoanions (R = Me, Ph) are essentially identical for all three counterions. Whereas the $[Na(THF)_2]^+$ and $[Li(THF)_3]^+$ salts crystallize such that the asymmetric unit in each compound contains a complete monoanion and cation, the $[(Ph_3P)_2N]^+$ salt crystallizes such that both the monoanion (Figure 1) and cation (Figure 2) are constrained to lie on a crystallographic twofold axis. The acyl monoanion in this latter salt thereby possesses a crystallographic disorder between two orientations such that the equatorial acyl ligand of one iron atom and an equatorial carbonyl ligand of the other iron atom are nearly superimposed in the twofold-averaged crystal structure. The C_2-2 conformation of the $[(Ph_3P)_2N]^+$ counterion (Figure 2) containing two identical P-N bond lengths of 1.556 (6) Å and a P-N-P′ bond angle of 157 (2)° is similar to those found[22] in several other $[(Ph_3P)_2N]^+$ salts.

In contrast to the solid-state structure of the $[(Ph_3P)_2N]^+$ salt, in the crystal structures of the $[Na(THF)_2]^+$ and

Table III. Least-Squares Planes for $[(Ph_3P)_2N]^+[Fe_2(CO)_5(C(O)Me)(\mu_2\text{-}PPh_2)_2]^-$

A. Equations Defining the Least-Squares Planes[a,b]

plane I, through P(1), P(1)^I, C(1), C(1-1)

$0.6586X + 0.6623Y - 0.3573Z + 11.3009 = 0$

plane II, through Fe, Fe^I, C(1-1)

$-0.3276X - 0.6996Y - 0.6350Z - 9.9431 = 0$

plane III, through C(1-1), O(1-1), C(2-1)

$-0.0175X - 0.5368Y - 0.8435Z - 6.4243 = 0$

B. Perpendicular Distances (Å) of Some Atoms from Each Plane

	I	II	III
Fe	0.34	0	−0.01
Fe^I	−1.69	0	−1.02
P	0.02	0.31	0.02
P^I	−0.02	−1.74	−2.15
C(1)	−0.02	1.71	1.75
C(2)	1.98	−0.81	−0.17
C(1-1)	0.02	0	0
O(1-1)	0.87	−0.40	0
C(2-1)	−1.12	0.40	0
C(3)	−0.75	0.19	−0.16

C. Angles (deg) between Normals to the Planes

	I	II	III
I		117	94
II			24

[a] The superscript (I) refers to the symmetry-related position $-1 - x, y, -z$. [b] The equations of the planes are given in an orthogonal ångstrom coordinate system (X, Y, Z) which is related to the fractional unit cell coordinate system (x, y, z) as follows: $X = xa$, $Y = yb$, $Z = zc$.

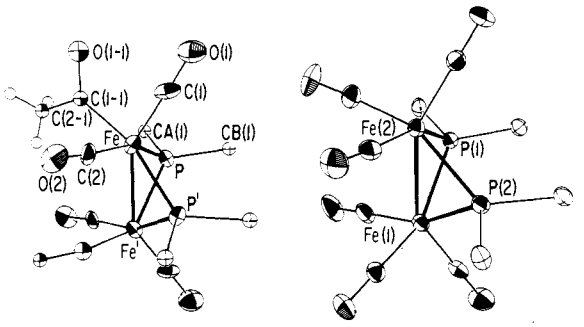

Figure 1. Configurations of the $[Fe_2(CO)_5(C(O)Me)(\mu_2\text{-}PPh_2)_2]^-$ monoanion (on the left) of the bis(triphenylphosphine)iminium salt and of the structurally related $Fe_2(CO)_6(\mu_2\text{-}PPh_2)_2$ (on the right). For clarity, only the phosphorus-attached phenyl carbon atoms are shown. Both Fe-Fe bonded dimers possess crystallographic C_2-2 site symmetry, which necessitates two equally weighted orientations in the crystalline state for the monoanion. Although the resulting disorder-averaged architecture (involving a near superposition of the acyl ligand of Fe and an equatorial carbonyl ligand of Fe′ due to their two half-weighted orientations related by the crystallographic twofold axis) precludes an accurate determination of its geometrical parameters, its overall structure was unambiguously resolved.

$[Li(THF)_3]^+$ salts there are strong interactions between the alkali metal ions and the monoanions. The sodium ion is observed in Figure 3 to form tight ion-pair interactions with the acyl oxygen atom and a carbonyl oxygen atom of one monoanion and with a carbonyl oxygen atom of another monoanion. Its additional interactions with two THF oxygen atoms give rise to a five-coordinate environment for the sodium ion. On the other hand, the lithium ion is shown in Figure 4 to form a strong ion pair with only the acyl oxygen atom of the monoanion with its tetrahedral-like oxygen environment being completed by coordination with three THF molecules. In the

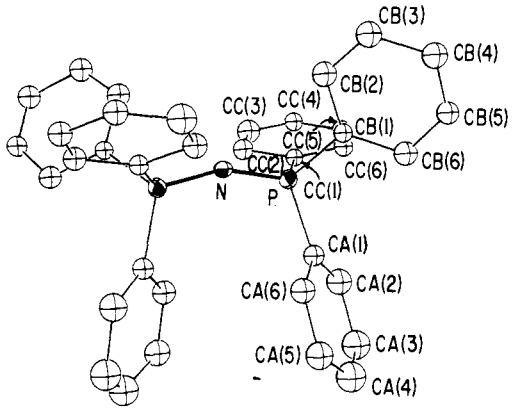

Figure 2. Conformation of the bis(triphenylphosphine)iminium cation of the $[Fe_2(CO)_5(C(O)Me)(\mu_2\text{-}PPh_2)_2]^-$ salt. This $[(Ph_3P)_2N]^+$ cation possesses a crystallographic twofold axis passing through the central nitrogen atom and bisecting the bent P-N-P fragment.

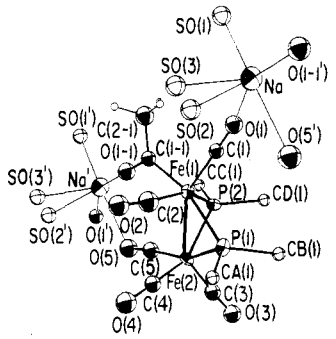

Figure 3. Configuration of the $[Fe_2(CO)_5(C(O)Me)(\mu_2\text{-}PPh_2)_2]^-$ monoanion showing its strong ion pairing to one Na^+ ion via the acyl oxygen atom of Fe(1) and one equatorial carbonyl oxygen atom of Fe(2) and to a symmetry-related Na^+ ion by an axial carbonyl oxygen atom of Fe(1). The independent Na^+ ion completes its five-coordinate oxygen environment (which may be regarded as a distorted square pyramid) by interactions with a crystalline-ordered THF molecule through its oxygen atom located at SO(1) and with a crystalline-disordered THF molecule through its oxygen atom randomly located in the apical position at either SO(2) or SO(3).

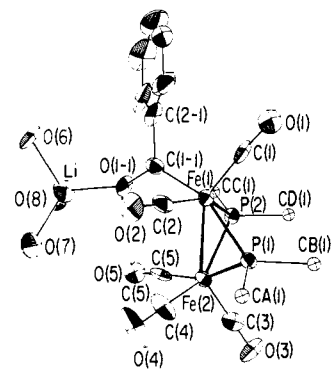

Figure 4. Configuration of the $[Fe_2(CO)_5(C(O)Ph)(\mu_2\text{-}PPh_2)_2]^-$ monoanion revealing its strong ion pairing in the crystalline state via an interaction of the acyl oxygen atom with a Li^+ which completes its tetrahedral coordination by interactions with the oxygen atoms of three THF molecules.

$[(Ph_3P)_2N]^+$ salt the outward orientation of the acyl oxygen atom may be determined by two weak hydrogen bonding O···H-C interactions with one phenyl hydrogen of the $[(Ph_3P)_2N]^+$ cation (corresponding to an O···C separation of 3.39 (3) Å) and with one phenyl hydrogen of a bridging di-

Table IV. Atomic Parameters[a] for $[Na(C_4H_8O)_2]^+[Fe_2(CO)_5(C(O)Me)(\mu_2\text{-}PPh_2)_2]^-$

	x	y	z	B, Å²		x	y	z	B, Å²
Fe(1)	0.2729(4)	0.1000(2)	0.2376(2)	*b*	CA(5)	0.5427	0.2533	0.1065	6.5
Fe(2)	0.0945(4)	0.1786(2)	0.2742(3)	*b*	CA(6)	0.4969	0.2176	0.1580	5.2
P(1)	0.3332(8)	0.1881(4)	0.2676(5)	*b*	HA(2)	0.2506	0.3006	0.2148	6.0
P(2)	0.1840(8)	0.1058(4)	0.3407(4)	*b*	HA(3)	0.3294	0.3621	0.1261	6.0
Na	0.7784(13)	0.0260(5)	0.2109(8)	*b*	HA(4)	0.5141	0.3322	0.0575	6.0
O(1)	0.5550(22)	0.0467(9)	0.2605(11)	4.93	HA(5)	0.6201	0.2407	0.0777	6.0
C(1)	0.4401(31)	0.0665(12)	0.2513(15)	3.18	HA(6)	0.5414	0.1792	0.1665	6.0
O(5)	−0.1948(27)	0.1274(9)	0.2430(14)	6.88	CB(1)	0.4581	0.2133	0.3479	2.5
C(5)	−0.0801(37)	0.1473(14)	0.2584(18)	5.04	CB(2)	0.4297	0.2634	0.3817	4.0
O(1-1)	0.0132(24)	0.0334(9)	0.1987(12)	5.90	CB(3)	0.5290	0.2839	0.4408	4.7
C(1-1)	0.1514(32)	0.0360(13)	0.2099(16)	3.74	CB(4)	0.6568	0.2542	0.4660	4.9
C(2-1)	0.2123(36)	−0.0203(15)	0.1968(19)	6.48	CB(5)	0.6852	0.2041	0.4322	6.1
O(2)	0.2304(24)	0.1179(9)	0.0843(14)	6.69	CB(6)	0.5858	0.1837	0.3731	5.0
C(2)	0.2460(40)	0.1121(16)	0.1491(24)	7.32	HB(2)	0.3375	0.2848	0.3635	6.0
O(3)	0.0547(24)	0.2618(10)	0.3807(13)	7.04	HB(3)	0.5085	0.3200	0.4652	6.0
C(3)	0.0641(36)	0.2268(16)	0.3335(21)	6.27	HB(4)	0.7284	0.2690	0.5086	6.0
O(4)	0.0098(25)	0.2280(10)	0.1302(14)	7.57	HB(5)	0.7774	0.1827	0.4504	6.0
C(4)	0.0511(37)	0.2093(15)	0.1915(22)	6.26	HB(6)	0.6063	0.1475	0.3488	6.0
SO(1)	0.7231(27)	−0.0676(11)	0.2047(14)	7.63	CC(1)	0.0530	0.0566	0.3717	3.2
SCA(1)	0.8049(50)	−0.1051(23)	0.1702(25)	11.3	CC(2)	−0.0627	0.0801	0.4006	4.8
SCA(2)	0.7757(51)	−0.1606(20)	0.1982(26)	11.2	CC(3)	−0.1641	0.0457	0.4267	5.6
SCA(3)	0.6734(54)	−0.1517(22)	0.2522(29)	12.6	CC(4)	−0.1498	−0.0123	0.4239	5.6
SCA(4)	0.6183(50)	−0.0957(22)	0.2415(26)	11.2	CC(5)	−0.0341	−0.0359	0.3950	7.2
H(1)	0.1514	−0.0407	0.1521	6.0[c]	CC(6)	0.0673	−0.0014	0.3689	5.0
H(2)	0.3280	−0.0174	0.1928	6.0	HC(2)	−0.0730	0.1220	0.4026	6.0
H(3)	0.2042	−0.0462	0.2467	6.0	HC(3)	−0.2476	0.0627	0.4476	6.0
SO(2)[d]	0.6937	0.0601	0.0899	8.0	HC(4)	−0.2231	−0.0371	0.4427	6.0
SCB(1)	0.7907	0.0852	0.0526	11.5	HC(5)	−0.0238	−0.0778	0.3929	6.0
SCB(2)	0.5583	0.0654	0.0493	11.5	HC(6)	0.1508	−0.0185	0.3480	6.0
SCB(3)	0.5715	0.0938	−0.0132	11.5	CD(1)	0.3030	0.1128	0.4286	2.5
SCB(4)	0.7151	0.1061	−0.0112	11.5	CD(2)	0.2825	0.1548	0.4785	4.0
SO(3)	0.6936	0.0329	0.0793	8.0	CD(3)	0.3731	0.1576	0.5466	6.1
SCC(1)	0.6404	0.0861	0.0763	11.5	CD(4)	0.4843	0.1183	0.5650	4.3
SCC(2)	0.7088	0.1158	0.0291	11.5	CD(5)	0.5048	0.0763	0.5151	5.8
SCC(3)	0.8042	0.0811	0.0028	11.5	CD(6)	0.4142	0.0736	0.4470	5.0
SCC(4)	0.7949	0.0298	0.0339	11.5	HD(2)	0.2022	0.1831	0.4652	6.0
CA(1)	0.3896	0.2350	0.1978	4.0	HD(3)	0.3583	0.1878	0.5826	6.0
CA(2)	0.3281	0.2881	0.1861	5.6	HD(4)	0.5497	0.1203	0.6142	6.0
CA(3)	0.3738	0.3238	0.1345	6.8	HD(5)	0.5851	0.0480	0.5284	6.0
CA(4)	0.4811	0.3064	0.0947	5.7	HD(6)	0.4290	0.0433	0.4110	6.0

Rigid-Body Parameters[d]

group	x	y	z	φ	θ	ρ	B, Å²
THF-B	0.654(5)	0.076(1)	0.045(2)	−0.43(9)	2.15(4)	0.58(9)	−0.6(9)
THF-C	0.718(8)	0.094(2)	0.036(4)	2.99(7)	−2.71(6)	0.59(6)	2.9(9)
C_6H_5(A)	0.4354(13)	0.2707(6)	0.1463(7)	−2.36(1)	2.93(1)	0.76(1)	0.0(−)
C_6H_5(B)	0.5574(14)	0.2338(5)	0.4070(7)	−2.48(1)	3.08(1)	−0.88(1)	0.0(−)
C_6H_5(C)	−0.0484(14)	0.0221(6)	0.3978(6)	−2.55(1)	2.90(1)	−2.78(1)	0.0(−)
C_6H_5(D)	0.3936(12)	0.1156(5)	0.4968(7)	−2.54(1)	2.90(1)	−1.16(1)	0.0(−)

	β_{11}	β_{22}	β_{33}	β_{12}	β_{13}	β_{23}		β_{11}	β_{22}	β_{33}	β_{12}	β_{13}	β_{23}
Fe(1)	64	16	23	2	15	−1	P(2)	85	13	30	1	29	0
Fe(2)	70	16	29	8	10	2	Na	78	33	64	−9	28	−6
P(1)	83	22	25	−7	19	−3							

[a] The estimated standard deviations of the least significant figures are given in parentheses. [b] Anisotropic temperature factors of the form $\exp\{-[\beta_{11}h^2 + \beta_{22}k^2 + \beta_{33}l^2 + 2\beta_{12}hk + 2\beta_{13}hl + 2\beta_{23}kl]\}$ were used. The resulting anisotropic temperature factors, β_{ij} ($\times 10^4$), are listed. [c] Hydrogen atoms were assigned fixed thermal and positional parameters throughout the least-squares refinement. [d] For the crystal-disordered THF molecule, each of its two determined orientations labeled THF-B (comprised of SO(2), SCB(1)-SCB(4)) and THF-C (comprised of SO(3), SCC(1)-SCC(4)) was half-weighted. The THF-B and THF-C rings were refined as rigid groups with hydrogens excluded. Each individual atom in the group was assigned an isotropic thermal parameter equivalent to the average of the corresponding values on the well-behaved solvent molecule. Only the group thermal parameter was varied in the final least-squares cycles. Each ring was assumed to have D_{5h} symmetry with a C-C bond length of 1.46 Å. All phenyl groups were refined as rigid groups, including hydrogen atoms. The individual isotropic thermal parameter on each carbon atom in the group was allowed to vary during the refinement. Each ring was assumed to have D_{6h} symmetry with a C-C bond of 1.39 Å and a C-H bond of 1.08 Å. In each of the two types of groups, the origin is at the center of the carbon (and oxygen) framework. The orthonormal set (x', y', z') has x' along C(1)-C(4), y' along the perpendicular bisector of C(2)-C(3), and z' along x' cross y'.

phenylphosphido ligand (corresponding to an O···C separation of 3.30 (4) Å). These large O···C separations imply at most only weak hydrogen-bonding interactions with the acyl oxygen atom.

From the occurrence of strong ion pairing between the alkali metal ion and the acyl oxygen atom in the $[Na(THF)_2]^+$ and $[Li(THF)_3]^+$ salts, it is evident that any possible coordination of the acyl oxygen atom to the second iron atom in an acyl

Table V. Interatomic Distances and Angles[a] for $[Na(C_4H_8O)_2]^+[Fe_2(CO)_5(C(O)Me)(\mu_2\text{-}PPh_2)_2]^-$

A. Distances (Å)

Fe(1)-Fe(2)	2.664(6)	Fe(2)-C(5)	1.76(3)	C(1-1)-O(1-1)	1.27(3)	Na′-O(1-1)	2.23(2)
P(1)···P(2)	2.865(12)	C(1)-O(1)	1.15(3)	C(1-1)-C(2-1)	1.49(4)	Na′-SO(1′)	2.29(3)
Fe(1)-P(1)	2.226(10)	C(2)-O(2)	1.19(4)	O(1-1)···C(2-1)	2.26(4)	Na′-SO(2′)	2.38
Fe(1)-P(2)	2.196(9)	C(3)-O(3)	1.22(4)	P(1)-CA(1)	1.84	Na′-SO(3′)	2.43
Fe(2)-P(1)	2.250(8)	C(4)-O(4)	1.22(4)	P(1)-CB(1)	1.82	SO(1)-SCA(1)	1.39(4)
Fe(2)-P(2)	2.210(10)	C(5)-O(5)	1.16(3)	P(2)-CC(1)	1.85	SCA(1)-SCA(2)	1.46(5)
Fe(1)-C(1)	1.73(3)	Fe(1)-C(1-1)	1.92(3)	P(2)-CD(1)	1.81	SCA(2)-SCA(3)	1.50(5)
Fe(1)-C(2)	1.64(4)	Fe(1)···O(1-1)	2.88(2)	Na′-O(5)	2.50(2)	SCA(3)-SCA(4)	1.43(6)
Fe(2)-C(3)	1.64(4)	Fe(1)···C(2-1)	3.00(4)	Na′-O(1′)	2.45(2)	SCA(4)-SO(1)	1.44(4)
Fe(2)-C(4)	1.68(4)	Fe(2)···O(1-1)	3.77(2)				

B. Angles (deg)

Fe(1)-P(1)-Fe(2)	74.4(3)	P(1)-Fe(2)-C(5)	157(1)
Fe(1)-P(2)-Fe(2)	73.0(3)	P(2)-Fe(2)-C(4)	149(1)
P(1)-Fe(1)-P(2)	80.8(4)	C(4)-Fe(2)-C(5)	88(2)
P(1)-Fe(2)-P(2)	79.9(4)	P(1)-Fe(2)-C(4)	90(1)
P(1)-Fe(1)-C(1-1)	159(1)	P(2)-Fe(2)-C(5)*	91(1)
P(2)-Fe(1)-C(2)	146(1)	C(3)-Fe(2)-P(1)	104(1)
C(2)-Fe(1)-C(1-1)	84(2)	C(3)-Fe(2)-P(2)	106(1)
P(1)-Fe(1)-C(2)	94(1)	C(3)-Fe(2)-C(4)	105(2)
P(2)-Fe(1)-C(1-1)	90(1)	C(3)-Fe(2)-C(5)	99(2)
C(1)-Fe(1)-P(1)	103(1)	Fe(1)-C(1)-O(1)	177(3)
C(1)-Fe(1)-P(2)	111(1)	Fe(1)-C(2)-O(2)	176(4)
C(1)-Fe(1)-C(2)	102(1)	Fe(2)-C(3)-O(3)	174(3)
C(1)-Fe(1)-C(1-1)	98(1)	Fe(2)-C(4)-O(4)	174(3)
Fe(1)-C(1-1)-O(1-1)	128(2)	Fe(2)-C(5)-O(5)	175(3)
Fe(1)-C(1-1)-C(2-1)	123(2)	Na-O(1)-C(1)	148(2)
C(2-1)-C(1-1)-O(1-1)	109(3)	Na′-O(5)-C(5)	121(2)
Fe(1)-P(1)-CA(1)	119	Na′-O(1-1)-C(1-1)	165(2)
Fe(1)-P(1)-CB(1)	128	SO(1)-Na-O(1′)	91(1)
Fe(2)-P(1)-CA(1)	120	SO(2′)-Na′-O(1-1)	93
Fe(2)-P(1)-CB(1)	119	SO(2′)-Na′-O(5)	84
CA(1)-P(1)-CB(1)	99	SO(2′)-Na′-SO(1′)	105
Fe(1)-P(2)-CC(1)	126	SO(3′)-Na′-O(1-1)	93
Fe(1)-P(2)-CD(1)	121	SO(3′)-Na′-O(5)	100
Fe(2)-P(2)-CC(1)	118	SO(3′)-Na′-O(1′)	102
Fe(2)-P(2)-CD(1)	123	SO(3′)-Na′-SO(1′)	89
CC(1)-P(2)-CD(1)	97	Na-SO(1)-SCA(1)	121(3)
O(1-1)-Na′-O(5)	83(1)	Na-SO(1)-SCA(4)	126(3)
O(1-1)-Na′-SO(1′)	107(1)	SO(1)-SCA(1)-SCA(2)	106(4)
O(1-1)-Na′-O(1′)	157(1)	SCA(1)-SCA(2)-SCA(3)	106(4)
O(5)-Na′-O(1′)	77(1)	SCA(2)-SCA(3)-SCA(4)	107(4)
O(5)-Na′-SO(1′)	166(1)	SCA(3)-SCA(4)-SO(1)	107(4)
		SCA(4)-SO(1)-SCA(1)	112(4)

[a] All primed atoms refer to the symmetry-related position $-1 + x, y, z$.

monoanion (corresponding to I in the Introduction) would be definitely inhibited by a competitive ion-pair interaction with the alkali metal ion. Hence, the remote possibility for achieving such an interaction in the crystalline state and/or in solution would appear to be optimized in the absence of ion pairing by use of either the $[(Ph_3P)_2N]^+$ counterion or the $[M(2,2,2\text{-crypt})]^+$ counterion ($M = Na^+, K^+$)[2,23] where the alkali metal ion is completely enclosed by the cryptand ligand. The fact that in the $[(Ph_3P)_2N]^+$ salt the overall architecture of the binuclear iron acyl monoanion (corresponding to II) is analogous to those in the $[Na(THF)_2]^+$ and $[Li(THF)_3]^+$ salts makes it highly unlikely that I can be isolated in preference to II. It is noteworthy that the proposed structure I, in which the electron-pair Fe–Fe bond is ruptured upon coordination of the acyl oxygen atom to the second iron atom, gives rise to five coordination for one iron and six coordination for the other iron atom in contrast to the observed six coordination for both iron atoms in II.

Stereochemical and Bonding Consequences Arising from the Net Replacement of an Equatorial Carbonyl Ligand in $Fe_2(CO)_6(\mu_2\text{-}PPh_2)_2$ by a $C(O)R^-$ Ligand. The configurations of the $[Fe_2(CO)_5(C(O)R)(\mu_2\text{-}PPh_2)_2]^-$ monoanions (Figures 1, 3, and 4) closely resemble that of the neutral (Fe–Fe)-bonded $Fe_2(CO)_6(\mu_2\text{-}PPh_2)_2$[24] (Figure 1). In each monoanion the iron atom linked to the acyl ligand has a localized square-pyramidal ligand environment with the acyl carbon atom, one carbonyl carbon atom, and the two bridging phosphorus atoms comprising the equatorial ligands and a carbonyl carbon atom of the axial ligand. The iron atom is perpendicularly displaced by 0.34–0.45 Å out of the mean basal plane toward the axial carbonyl ligand. The binuclear iron acyl monoanion formally arises from the junction of the basal planes of two square pyramids along the nonbonding P···P edge. The existence of an electron pair Fe–Fe bond, which accounts for the diamagnetic character of the compounds, is in accord with the Fe–Fe distance of range 2.664 (6)–2.718 (5) Å in the three monoanions being analogous to the electron-pair Fe–Fe bonding distance of 2.623 (2) Å found in the neutral $Fe_2(CO)_6(\mu_2\text{-}PPh_2)_2$ dimer. The other mean geometrical parameters of the three monoanions also closely parallel those of the neutral $Fe_2(CO)_6(\mu_2\text{-}PPh_2)_2$ dimer. For example, the highly acute Fe(1)–P–Fe(2) bond angles, which have been attributed[25] to the strength of the Fe–Fe bond in the neutral $Fe_2(CO)_6(\mu_2\text{-}X)_2$-type dimer (e.g., X = NR_2, PR_2, SR), vary from 73.7 to 75.3° in the three monoanions compared to 72.0° in the neutral diphenylphosphido-bridged dimer.

Table VI. Least-Squares Planes[a] for $[Na(C_4H_8O)_2]^+[Fe_2(CO)_5(C(O)Me)(\mu_2\text{-}PPh_2)_2]^-$

A. Equations Defining the Least-Squares Planes[b]

plane I, through P(2), P(1), C(1-1), C(2)
$-0.8568X + 0.4386Y - 0.2712Z + 1.2259 = 0$

plane II, through P(2), P(1), C(4), C(5)
$0.2094X - 0.6897Y - 0.6931Z + 5.9434 = 0$

plane III, through O(1-1), C(1-1), C(2-1)
$0.1447X + 0.2362Y - 0.9609Z + 3.3519 = 0$

plane IV, through Fe(1), Fe(2), C(1-1)
$-0.0142X + 0.3214Y - 0.9468Z + 3.3476 = 0$

plane V, through O(1)[1], O(1-1), O(5), SO(1)[1]
$-0.2283X + 0.1764Y - 0.9575Z + 3.1636 = 0$

B. Perpendicular Distances (Å) of Some Atoms from the Designated Planes

	I	II	III	IV	V
Fe(1)	−0.45	1.68	0.03	0	
Fe(2)	1.70	−0.44	−0.42	0	
P(1)	−0.08	−0.05	0.07	0.15	
P(2)	0.08	0.05	−1.90	−1.71	
C(1)	−2.16		−0.18	−0.51	
C(2)	0.09		1.65	1.62	
C(3)		−2.08		−0.64	
C(4)		0.06		1.66	
C(5)		−0.06		0.05	
C(1-1)	−0.09		0	0	
C(2-1)	−1.13		0	−0.21	
O(1-1)	1.01		0	0.19	−0.05
O(1)[1]			−1.64	−0.71	−0.05
O(5)			−0.54	0.18	0.05
SO(1)[1]			−1.07	−0.65	0.04
Na[1]			−0.58	−0.04	0.22

C. Angles between Normals to the Planes (deg)

	I	II	III	IV	V
I		107	76	66	58
II			58	64	60
III				10	22
IV					15

[a] The superscript (1) refers to the symmetry-related position $-1 + x, y, z$. [b] The equations of the planes are given in an orthogonal ångstrom coordinate system (X, Y, Z) which is related to the fractional unit cell coordinate system (x, y, z) as follows: $X = xa + zc \cos\beta$, $Y = yb$, $Z = zc \sin\beta$.

The formal substitution of an electronically equivalent $C(O)R^-$ ligand in place of an equatorial carbonyl ligand in $Fe_2(CO)_6(\mu_2\text{-}PPh_2)_2$ lowers the symmetry from C_{2v}-2*mm* to C_1-1. The resulting asymmetry between the localized environments of the two nonequivalent iron atoms in the monoanion is not observed in the $[(Ph_3P)_2N]^+$ salt (other than the resolved half-weighted acyl ligand vs. the half-weighted equatorial carbonyl ligand) owing to the crystallographically-imposed twofold crystal disorder. Although the relatively large esd's in the $[Na(THF)_2]^+$ salt also preclude a meaningful comparison of corresponding distances and bond angles, for the $[Li(THF)_3]^+$ salt the determined variations in bond lengths and angles (which possess much lower esd's) reveal that the other ligands are affected by the formal replacement of an equatorial carbonyl ligand with a negatively charged acyl ligand. The iron atom, Fe(1), bonded to the acyl ligand is found to have *shorter* Fe-CO(equatorial), Fe-CO(axial), and Fe-P bond lengths than those for the iron atom, Fe(2)—viz., Fe-CO(equatorial), 1.767 (14) Å for Fe(1) vs. 1.783 (14) and 1.784 (14) Å for Fe(2); Fe-CO(axial), 1.722 (15) Å for Fe(1) vs. 1.744 (13) Å for Fe(2); Fe-P, 2.204 (3) and 2.206 (3) Å for Fe(1) vs. 2.248 (3) and 2.232 (3) Å for Fe(2). The latter Fe-P values are analogous to the Fe-P bond lengths of mean 2.233 Å and range 2.228 (3)-2.240 (3) Å found[24] in the $Fe_2(CO)_6(\mu_2\text{-}PPh_2)_2$ dimer. Despite the Fe-CO differences being nonsignificant from a statistical viewpoint, this bond-length trend for both the Fe-P and Fe-CO bonds is completely consistent with the notion that the replacement of one equatorial carbonyl ligand on Fe(1) by the much poorer π-acceptor $C(O)R^-$ ligands (vide infra) localizes more negative charge on Fe(1) which in turn results in a relatively greater π back-bonding from Fe(1) to its two CO and two P ligands. It is noteworthy that the observed infrared frequencies in the carbonyl region for $Fe_2(CO)_6(\mu_2\text{-}PPh_2)_2$ are 65-80 cm^{-1} higher than the corresponding ones for $[Li(THF)_3]^+[Fe_2(CO)_5(C(O)Ph)(\mu_2\text{-}PPh_2)_2]^-$.[26,27] Although this correlation is consistent with greater $d_\pi(Fe) \rightarrow \pi^*(CO)$ back-bonding in the monoanion than in the neutral parent, such a trend is not unexpected from charge considerations.

The Acyl Ligand. A. Its Geometry and Mode of Interaction with the Metal Atom. An examination of bond angles and least-squares planes expectedly shows the acyl carbon atom in each of the three $[Fe_2(CO)_5(C(O)R)(\mu_2\text{-}PPh_2)_2]^-$ monoanions to have an essentially coplanar trigonal arrangement with its three nearest neighbors—viz., O(1-1), Fe(1), and the methyl or phenyl C(2-1) atom.

The Fe-C(acyl) bond lengths of 1.990 (12), 1.92 (3), and 1.96 (3) Å in the $[Li(THF)_3]^+$, $[Na(THF)_2]^+$, and $[(Ph_3P)_2N]^+$ salts, respectively, are statistically equivalent. The much more precise value for the $[Li(THF)_3]^+$ salt, which is 0.2 Å longer than the 1.767 (14)-1.784 (14) Å range for the three terminal Fe-CO(equatorial) bond lengths in the monoanion, is also significantly longer than the value of 1.945 (6) Å for the Fe-C(bridged benzoyl) bond in III[4] but compares favorably with values for terminal acyl ligands such as the Fe-C(benzoyl) bond length of 1.97 (2) Å in $Fe(\eta^5\text{-}C_5H_5)(CO)(PPh_3)(C(O)Ph)$,[28] the Fe-C(acetyl) bond length of 1.968 (5) Å in $Fe(HBpz_3)(CO)_2(C(O)Me)$ (where $HBpz_3$ denotes the tridentate tris(1-pyrazolylborate) ligand, $HB(N_2C_3H_3)_3$),[29] the Fe-C(benzoyl) bond length of 1.93 (4) Å in Fe(DPPE)$(\eta^5\text{-}C_5H_5)(C(O)Ph)$ (where DPPE denotes the bidentate diphos ligand, $Ph_2PC_2H_4PPh_2$),[30] and the Fe-C(propenoyl) bond length of 1.979 (5) Å in dicarbonyl-3-$[\eta^5$-(2-cyclohexadienyl)]-σ-propenoyliron.[31] It is not surprising that these Fe-C(acyl) distances are all significantly shorter than the Fe-C(phenyl) bond length of 2.11 (2) Å in $Fe(\eta^5\text{-}C_5H_5)(CO)(PPh_3)(C_6H_5)$[32] and Fe-C(propyl) bond length of 2.20 (2) Å in $[(Ph_3P)_2N]^+[Fe(CO)_4(C_3H_7)]^-$.[22c] The considerably shorter Fe-C(acyl) bonds were attributed by Struchkov and co-workers[28] to $d_\pi(Fe) \rightarrow p_\pi(C)$ back-bonding in accord with similar bond-length evidence first presented by Churchill and Fennessey,[33] who concluded (on the basis of the Mo-C(acetyl) bond in $Mo(\eta^5\text{-}C_5H_5)(CO)_2(PPh_3)(C(O)Me)$ being 0.12 Å shorter than the Mo-C(methyl) bond in $[Mo(\eta^5\text{-}C_{10}H_8)(CO)_3Me]_2$[34]) that significant $d_\pi(\text{metal}) \rightarrow p_\pi(\text{acyl})$ back-bonding exists in transition metal-acyl complexes.

The planar acyl ligand of the $[Fe_2(CO)_5(C(O)R)(\mu_2\text{-}PPh_2)_2]^-$ monoanion in both the $[Li(THF)_3]^+$ and $[(Ph_3P)_2N]^+$ salts is approximately perpendicular (viz., 93 and 94°, respectively) to the plane of the other three iron-attached equatorial atoms such that Fe-C(acyl) multiple bond character is optimized within the equatorial plane. The acyl ligand in the $[Na(THF)_2]^+$ salt is somewhat tilted with respect to the equatorial plane of one carbonyl carbon and two phosphorus atoms (i.e., the angle between the normals of the two planes is 76°), presumably because of steric requirements imposed in part by the sodium cation interacting with both the acyl oxygen atom and an oxygen atom of an equatorial carbonyl ligand coordinated to the other iron atom. Although the bond-length data indicate that the acyl monoanions possess some degree of Fe-C(acyl) multiple-bond character, it appears not to be a dominant feature. In this connection, it is note-

worthy that Cotton et al.[29] pointed out that the σ component in the Fe-C(acetyl) bond in $Fe(HBpz_3)(CO)_2(C(O)Me)$ must be stronger and more dominant than that in the Fe-CO bonds in accord with the observed differences in the Fe-N bond lengths. Comparative MO calculations performed by Block, Fenske, and Casey[35] on both a metal acyl complex, $Mn(CO)_5(C(O)Me)$, and a corresponding metal carbene complex, $Cr(CO)_5(C(OMe)Me)$, substantiated the much greater σ-donor ability of an acetyl ligand which also was found to be a better σ donor but a poorer π acceptor than the carbene ligand. They concluded that the reactions of nucleophiles with either the metal acetyl or carbene complex would be frontier controlled rather than charge controlled with the differences in the energies and localization properties of the LUMOs of the two compounds indicating that attack of nucleophiles at carbonyl ligands is much more likely for the metal carbonyl acyl complex than for the metal carbonyl carbene complex.[36,37] These nonparametrized calculations[35] also indicated in harmony with resonance forms that the oxygen atom of an acyl complex is a better π donor to the carbon atom than the methoxy oxygen of the carbene complex.

B. Its Mode of Interaction with Alkali Metal Ions vs. That with an R^+ Substituent (Carbene Formation) or a Second Metal Atom (Acyl-Bridged Formation). Of prime interest is that the nature of interaction of the oxygen atom of the metal-acyl ligand with the alkali metal ion in both the $[Li(THF)_3]^+$ and $[Na(THF)_2]^+$ salts is completely different from that of the oxygen atom of the metal-acyl ligand in its interaction with either an R^+ substituent to give a metal-carbene complex[38,39] or a second metal atom to give an acyl-bridged binuclear metal complex such as **III**[4] or **IV**.[5] Both of these latter type of interactions involve an electron-pair donation from a normally $sp^2(O)$ orbital of the trigonal oxygen atom within the σ framework of the metal-acyl ligand. This particular mode of interaction is reflected in a metal alkoxycarbene complex or in III and IV by the resulting oxygen-coordinated carbon or metal atom being approximately coplanar with the metal-acyl ligand.

In sharp contrast, an inspection of the directional character of the Li^+-O(acyl) interaction in the $[Li(THF)_3]^+$ salt (Figures 4 and 5) shows the Li^+ ion to be situated 0.67 Å above the acyl O(1-1)-C(1-1)-C(2-1) plane in such an orientation that the resulting Li-O(1-1)-C(1-1) angle is 149°. Likewise, an examination of the $[Na(THF)_2]^+$ salt (Figure 3) reveals that the Na^+ ion forms a similar kind of contact ion pair with the acyl oxygen atom, as evidenced by its being located 0.58 Å above the acyl O(1-1)-C(1-1)-C(2-1) plane in such a direction to give a Na-O(1-1)-C(1-1) angle of 165°. Furthermore, a detailed analysis of the structural features of $[Li(THF)_3]^+[Fe_2(CO)_5(C(O)Ph)(\mu_2\text{-}PPh_2)_2]^-$ is especially informative in that the nearly regular tetrahedral oxygen arrangement about the Li^+ ion, as manifested by the six O-Li-O angles varying from 103 (2) to 113 (2)°, enables one to discern the nature of the Li^+-O(acyl) interaction. This analysis, presented in Figure 5, shows that within experimental error[40] a tetrahedral sp^3(Li) orbital would point directly at the acyl oxygen atom, O(1-1), with virtually no interaction with either the π(O-C) orbital or one of the two lone-pair sp^2(O) orbitals. It then follows that there is no evidence for any "covalency" in the Li^+-O(1-1) interaction involving a charge transfer from an orbital of the trigonal oxygen atom. The tight ion pairing between the Li^+ ion and its tetrahedral oxygen neighbors including O(1-1) may be readily attributed to the high electrostatic field strength of the Li^+ ion which is presumed to produce a charge polarization of the acyl ligand with an enhanced negative charge localized on the O(1-1) atom.

Another distinguishing feature between the different modes of interaction of an acyl oxygen atom with an alkali metal ion from that with an R^+ substituent or second metal atom is the

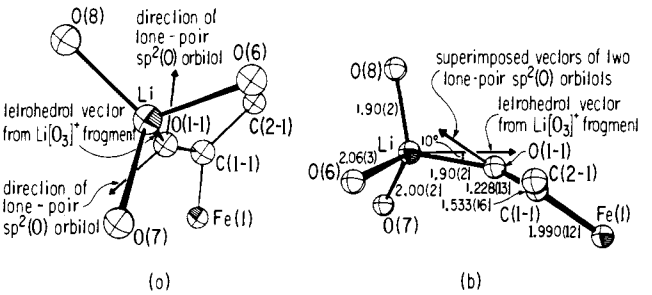

Figure 5. Two views showing the geometrical disposition of the trigonal-pyramidal $Li[O_3]^+$ fragment relative to the trigonal-planar RC(O)Fe fragment. An idealized tetrahedral vector from the $Li[O_3]^+$ fragment, constructed from the line passing through the Li^+ and the centroid of the three THF oxygen atoms, is found within experimental error (i.e., within 10°) to point directly at the trigonal O(1-1) atom. It is concluded from the relative orientations of the two fragments that there is no covalent interaction of an sp^3(Li) orbital along the tetrahedral direction with either the π(O-C) orbital or one of the two in-plane sp^2(O) orbitals. The almost regular tetrahedral oxygen environment about the Li^+ ion is then deemed to be a consequence of tight ion-pair packing. Hence, the high electrostatic field strength of the Li^+ ion is presumed to cause a strong charge polarization of the acyl ligand involving a net charge displacement from the acyl carbon atom, C(1-1), to the acyl O(1-1) atom (and concomitantly less π bonding with a slight lengthening of the C-O bond) without any charge transfer to the Li^+ ion (i.e., no Li-O(acyl) covalency).

resulting effect on the C-O bond length. The relatively tight Li^+-O(1-1) ion pair does not appear to markedly lengthen the C(1-1)-O(1-1) bond of a metal-C(acyl) ligand in that the observed value of 1.228 (13) Å in the $[Li(THF)_3]^+$ salt is comparable with a normal double-bond length of 1.216 (2) Å in acetophenone (at 154 K)[41] as well as with the determined C-O bond lengths in other metal acyl complexes including $Fe(\eta^5\text{-}C_5H_5)(CO)(PPh_3)(C(O)Ph)$ (1.22 (3) Å),[28] $Fe(HBpz_3)(CO)_2(C(O)Me)$ (1.193 (6) Å),[29] $Fe(\eta^5\text{-}C_6H_6CH{=}CHC(O))$ (1.208 (6) Å),[31] and $Mo(\eta^5\text{-}C_5H_5)(CO)_2(PPh_3)(C(O)Me)$ (1.211 (16) Å).[33]

On the other hand, significantly longer C-O bond lengths in the range 1.30-1.33 Å have been reported[42] for a number of metal alkoxycarbene complexes, while intermediate C-O bond lengths are found in III and IV—viz., two crystallographically equivalent values of 1.262 (8) Å in III[4] and two crystallographically independent values of 1.257 (10) and 1.258 (10) Å in IV.[5] It is apparent that π bonding in a metal acyl complex is predominantly within the C-O bond rather than in the M-C(acyl) bond. The longer C-O bond lengths in metal alkoxycarbene complexes and in III and IV are primarily a consequence of less π bonding between the carbon and oxygen atoms. This decreased π-electron delocalization from the oxygen atom is due to partial charge transfer from the oxygen atom to the R^+ or second metal atom via the electron-donating sp^2(O) orbital. In turn, π back-bonding from the metal to the carbon atom is enhanced by the opposing effect of π(C-O) bonding being decreased.

Oxygen Coordination about the Li^+ and Na^+ Ions and Resulting Implications. A further examination of the solid-state coordination of oxygen atoms with the alkali metal ions provides an indication of the relative extent of ion pairing. For the nearly regular tetrahedral oxygen environment about the Li^+ ion in $[Li(THF)_3]^+[Fe_2(CO)_5(C(O)Ph)(\mu_2\text{-}PPh_2)_2]^-$ (Figures 4 and 5), the tight Li^+-O(acyl) interaction is reflected by its distance of 1.902 (25) Å being as short or shorter than those of 1.905 (25), 2.002 (24), and 2.063 (27) Å for the three Li^+-O(THF) interactions. The absence of any direct Li^+-O(carbonyl) interactions may be attributed to their relative strength being considerably less than that for the Li^+-O(THF) interaction. This preference in the solid state for Li^+-O(THF) interactions rather than Li^+-O(carbonyl) interactions is in

Table VII. Atomic Parameters for $[Li(C_4H_8O)_3]^+[Fe_2(CO)_5(C(O)Ph)(\mu_2\text{-}PPh_2)_2]^-$

atom	10^4x	10^4y	10^4z	$10^4\beta_{11}$	$10^4\beta_{22}$	$10^4\beta_{33}$	$10^4\beta_{12}$	$10^4\beta_{13}$	$10^4\beta_{23}$
Fe(1)	2974(1)	2500(0)	2439(1)	60(1)	23(1)	49(1)	6(2)	2(2)	2(1)
Fe(2)	1450(1)	2932(1)	3997(1)	64(1)	24(1)	56(1)	1(2)	2(2)	−7(2)
P(1)	3290(3)	2257(2)	4113(2)	70(3)	21(1)	47(2)	3(3)	3(4)	−2(2)
P(2)	1014(3)	2073(2)	2793(2)	68(3)	22(1)	50(2)	−7(3)	−5(4)	1(3)
Li	1226(20)	4587(10)	0836(19)	109(21)	37(8)	129(18)	34(28)	38(36)	1(19)
O(1)	4313(9)	1248(5)	1558(7)	189(13)	39(3)	117(8)	68(11)	65(18)	−29(9)
C(1)	3743(11)	1760(7)	1876(9)	86(10)	41(5)	60(8)	6(8)	14(17)	32(10)
O(2)	4898(9)	3673(5)	2362(7)	131(10)	39(3)	118(8)	−55(9)	−14(16)	−2(9)
C(2)	4151(11)	3210(6)	2406(9)	95(11)	30(4)	62(8)	23(9)	3(19)	−11(9)
O(1-1)	1582(8)	3611(4)	1293(6)	129(10)	37(3)	62(5)	41(9)	7(14)	24(7)
C(1-1)	2230(10)	3046(6)	1219(8)	96(10)	27(4)	63(8)	−10(9)	14(17)	−11(9)
C(2-1)	2497(12)	2777(7)	0106(8)	143(11)	44(6)	49(7)	−2(15)	−55(16)	27(9)
O(3)	0187(7)	2543(6)	5929(6)	115(9)	76(4)	65(5)	16(12)	11(13)	33(10)
C(3)	0651(9)	2691(7)	5141(9)	52(10)	44(6)	79(9)	27(12)	−20(17)	−14(10)
O(4)	2979(9)	4236(5)	4562(11)	117(11)	32(3)	316(15)	−40(11)	−78(18)	−40(13)
C(4)	2415(11)	3717(7)	4330(11)	58(10)	32(5)	164(14)	23(10)	44(19)	−29(11)
O(5)	−0476(9)	3945(5)	3109(7)	175(12)	42(3)	136(9)	99(9)	−40(19)	21(10)
C(5)	0254(11)	3535(6)	3435(9)	93(11)	36(5)	63(8)	6(8)	12(18)	−31(11)
CA(1)	0745(11)	1128(6)	3231(9)	100(14)	18(4)	69(8)	16(13)	12(17)	−3(10)
CA(2)	1468(13)	0561(7)	2882(10)	127(16)	29(4)	92(10)	−20(15)	−37(18)	36(13)
CA(3)	1222(15)	−0162(7)	3176(13)	177(17)	29(5)	162(16)	−8(17)	−25(26)	36(12)
CA(4)	0235(18)	−0305(7)	3840(12)	322(25)	23(4)	123(13)	−89(18)	−120(28)	34(12)
CA(5)	−0495(19)	0249(8)	4226(11)	365(27)	45(6)	95(12)	−144(20)	27(27)	37(13)
CA(6)	−0275(12)	0976(7)	3901(9)	146(19)	45(5)	66(9)	−55(18)	83(22)	−6(8)
CB(1)	−0393(9)	2114(6)	1894(8)	58(13)	27(4)	57(7)	−1(13)	11(17)	1(8)
CB(2)	−1595(11)	2386(8)	2134(9)	97(14)	56(6)	75(9)	8(16)	9(17)	−25(9)
CB(3)	−2655(12)	2329(10)	1499(11)	94(14)	95(9)	110(11)	46(21)	−27(18)	−58(16)
CB(4)	−2519(12)	2001(9)	0506(10)	104(14)	69(7)	100(11)	17(17)	−107(22)	2(15)
CB(5)	−1320(14)	1736(8)	0235(11)	134(17)	64(7)	93(11)	23(17)	−59(19)	−59(14)
CB(6)	−0293(11)	1796(7)	0915(10)	81(12)	50(5)	83(10)	−10(16)	−46(19)	−36(12)
CC(1)	4712(10)	2637(6)	4835(8)	98(13)	22(4)	60(8)	23(14)	−8(16)	−21(11)
CC(2)	5915(10)	2599(7)	4422(8)	58(10)	44(5)	74(8)	5(12)	−33(18)	14(12)
CC(3)	7024(12)	2816(8)	4984(9)	118(13)	63(7)	79(9)	15(16)	13(16)	−3(11)
CC(4)	6904(12)	3080(7)	5980(11)	116(13)	27(5)	136(12)	−2(16)	−65(17)	16(12)
CC(5)	5693(13)	3140(7)	6399(9)	146(15)	46(6)	75(9)	13(16)	−77(17)	−34(12)
CC(6)	4607(11)	2916(8)	5815(8)	100(12)	49(5)	61(8)	0(16)	12(16)	−17(11)
CD(1)	3359(11)	1337(6)	4689(8)	88(12)	32(4)	65(8)	11(14)	−58(17)	−27(12)
CD(2)	4285(14)	0855(7)	4324(10)	161(15)	34(5)	99(11)	10(16)	−48(12)	27(12)
CD(3)	4397(15)	0142(8)	4765(12)	218(17)	35(5)	132(13)	59(16)	−143(26)	−11(10)
CD(4)	3670(16)	−0070(8)	5561(11)	235(18)	38(5)	128(13)	−27(16)	−109(26)	63(13)
CD(5)	2684(16)	0404(8)	5908(12)	191(17)	59(6)	133(13)	−56(17)	−93(25)	89(17)
CD(6)	2566(13)	1004(6)	5479(9)	180(16)	30(4)	62(8)	−6(15)	−11(17)	50(12)
O(6)	1930(9)	5349(5)	1902(8)	184(13)	40(4)	19(8)	−23(12)	6(16)	−2(9)
C(37)	1202(18)	5698(10)	2746(13)	257(28)	78(9)	137(14)	−15(26)	176(27)	−57(21)
C(38)	2223(25)	6110(13)	3305(17)	542(48)	106(10)	219(22)	−277(38)	214(61)	−168(23)
C(39)	3450(19)	6086(12)	2842(14)	253(31)	103(10)	160(16)	−61(31)	50(39)	−134(21)
C(40)	3326(19)	5521(11)	1981(15)	238(29)	77(9)	168(18)	15(29)	47(39)	−44(19)
O(7)	2308(8)	4784(5)	−0422(6)	119(10)	56(4)	75(6)	28(12)	52(13)	45(8)
C(41)	1762(15)	4847(10)	−1446(11)	183(21)	75(8)	88(11)	60(20)	−24(31)	31(19)
C(42)	2894(18)	4812(13)	−2165(13)	229(29)	129(13)	102(13)	−49(29)	107(30)	6(18)
C(43)	3990(14)	4525(11)	−1526(12)	120(21)	94(9)	121(14)	4(22)	25(31)	−38(20)
C(44)	3706(13)	4755(10)	−0439(11)	116(21)	81(8)	107(12)	22(21)	72(21)	−40(20)
O(8)	−0597(11)	4723(8)	0569(9)	46(18)	71(11)	162(15)	22(31)	32(33)	48(22)
C(45)	8626(15)	4100(14)	0362(14)	97(24)	104(13)	319(19)	−21(32)	−71(38)	4(24)
C(48)	8574(16)	5313(15)	0772(14)	36(24)	90(15)	471(21)	90(32)	144(40)	70(24)
C(46-1)	7257(17)	4328(15)	0699(15)	12.1(1)					
C(46-2)	7268(16)	4297(16)	−0048(17)	13.4(2)					
C(47-1)	7328(17)	5067(16)	0948(16)	12.7(1)					
C(47-2)	7270(17)	4990(16)	0185(16)	10.3(1)					
HA(2)	2228	0667	2378	6.0					
HA(3)	1800	−0591	2924	7.0					
HA(4)	0035	−0834	4041	7.0					
HA(5)	−1256	0153	4767	7.0					
HA(6)	−0883	1400	4147	6.0					
HB(2)	−1705	2653	2826	5.0					
HB(3)	−3543	2499	1743	6.0					
HB(4)	−3305	1977	−0019	6.0					
HB(5)	−1238	1481	−0490	6.0					
HB(6)	0611	1619	0663	5.0					
HC(2)	6016	2416	3676	5.0					
HC(3)	7924	2760	4665	6.0					
HC(4)	7718	3249	6395	6.0					
HC(5)	5588	3357	7118	6.0					

Table VII (*Continued*)

atom	10^4x	10^4y	10^4z	$10^4\beta_{11}$	$10^4\beta_{22}$	$10^4\beta_{33}$	$10^4\beta_{12}$	$10^4\beta_{13}$	$10^4\beta_{23}$
HC(6)	3699	2972	6145	5.0					
HD(2)	4894	1015	3714	6.0					
HD(3)	5077	−0222	4493	7.0					
HD(4)	3843	−0553	5946	7.0					
HD(5)	2015	0210	6440	7.0					
HD(6)	1871	1464	5782	6.0					
H(2-2)	0572	3031	−0387	7.0					
H(2-3)	0932	2534	−2170	8.0					
H(2-4)	2946	1991	−2563	8.0					
H(2-5)	4806	2088	−1397	8.0					
H(2-6)	4482	2537	0339	7.0					

[a] Anisotropic thermal parameters of the form $\exp[-(\beta_{11}h^2 + \beta_{22}k^2 + \beta_{33}l^2 + 2\beta_{12}hk + 2\beta_{13}hl + 2\beta_{23}kl)]$ were used for all nonhydrogen atoms, except for two tetrahydrofuran carbon atoms, C(46-*n*) and C(47-*n*), which are randomly disordered between two positions $n = 1, 2$. For these latter half-weighed atoms as well as for the hydrogen atoms, the utilized isotropic temperature factors are given in a single column to the right of the atomic coordinates. [b] The phenyl hydrogen atoms were placed at idealized positions for a regular phenyl ring with C-H distances of ca. 1.0 Å. Their isotropic temperature factors were set to an integral value approximately 1 Å^2 more than those determined for their respective carbon atoms.

harmony with the findings in the solution state by the Darensbourgs and co-workers,[9b,d] who have carried out a comprehensive examination via infrared, kinetic, and conductivity measurements of solvent effects on alkali metal interactions with the *trans*-benzoyltricarbonyl(triphenylphosphine)iron(−I) monoanion[9b] and with derivatives of manganese carbonylates.[9d] In both cases, they found that a complete breakdown of the Li^+-O(carbonyl) ion pairing occurred in THF. They also pointed out[9d] that their observations are consistent with the increased stability of $Li^+ \cdot n$THF solvate over a $Na^+ \cdot n$THF solvate.

Each Na^+ ion in $[Na(THF)_2]^+[Fe_2(CO)_5(C(O)Me)(\mu_2\text{-}PPh_2)_2]^-$ may be regarded as possessing a distorted square-pyramidal environment of oxygen atoms (Figure 3), comprised of the acyl oxygen and one carbonyl oxygen from one monoanion, a carbonyl oxygen from a symmetry-related monoanion, and two oxygen atoms from the THF molecules. The relative strength of a Na^+-O interaction appears to be directly related to the observed distance with the shortest separation of 2.23 (2) Å occurring for the Na^+-O(acyl) interaction compared to the much longer values of 2.45 (2) and 2.50 (2) Å found for the two Na^+-O(carbonyl) interactions. One of the two Na^+-O(THF) interactions arises at a distance of 2.29 (3) Å from the oxygen atom, SO(1), of the crystallographically well-defined THF molecule which occupies the fourth square-pyramidal basal position. The apical oxygen atom of the poorly resolved THF molecule is disordered between two half-weighted sites, SO(2) and SO(3), which are 2.38 and 2.43 Å, respectively, from the Na^+ ion. Although it has been shown[43] that Na^+ ions contained in organic compounds generally prefer to be six coordinate in the solid state, it is presumed here that the bulky $[Fe_2(CO)_5(C(O)Me)(\mu_2\text{-}PPh_2)_2]^-$ monoanion, which effectively functions as a chelating ligand in linking Na^+ ions into an infinite-(cation-anion)$_n$-chain, sterically limits the coordination number of the Na^+ ion to five in the crystalline state.

In this connection, Chin and Bau[11a] found from their structural determination of $Na_2Fe(CO)_4 \cdot 1.5(C_4H_8O_2)$ that strong ion pairing originated from four short-range Na^+-O(carbonyl) interactions of 2.32 Å between an octahedrally coordinated Na^+ and four different $[Fe(CO)_4]^{2-}$ dianions along with two Na^+-O(dioxane) interactions of 2.339 (6) and 2.988 (6) Å. They also found the unanticipated existence of long-range Na···C and Na···Fe interactions of 2.95 and 3.09 Å, respectively, between another crystallographically independent Na^+ ion and the C-Fe-C portion of the $[Fe(CO)_4]^{2-}$ dianion which was proposed[11] to be mainly responsible for the large observed angular distortion of the dianion from a regular tetrahedral geometry (viz., with one OC-Fe-CO bond angle of 129.7 (2)°).

Table VIII. Interatomic Distances and Bond Angles for $[Li(C_4H_8O)_3]^+[Fe_2(CO)_5(C(O)Ph)(\mu_2\text{-}PPh_2)_2]^-$

A. Distances (Å)

Fe(1)-Fe(2)	2.670(2)	Fe(1)-C(1)	1.722(15)
Fe(1)-P(1)	2.204(3)	Fe(1)-C(2)	1.767(14)
Fe(1)-P(2)	2.206(3)	Fe(2)-C(3)	1.744(13)
Fe(2)-P(1)	2.248(3)	Fe(2)-C(4)	1.783(14)
Fe(2)-P(2)	2.232(3)	Fe(2)-C(5)	1.784(14)
P(1)···P(2)	2.869(4)		
		C(1)-O(1)	1.174(14)
Fe(1)-C(1-1)	1.990(12)	C(2)-O(2)	1.140(13)
Fe(1)···O(1-1)	2.861(8)	C(3)-O(3)	1.155(12)
Fe(1)···C(2-1)	3.056(8)	C(4)-O(4)	1.143(14)
Fe(2)···O(1-1)	3.678(8)	C(5)-O(5)	1.130(13)
C(1-1)-C(2-1)	1.533(16)		
C(1-1)-O(1-1)	1.228(13)	Li-O(1-1)	1.902(25)
O(1-1)···C(2-1)	2.353(13)	Li-O(6)	2.063(27)
		Li-O(7)	2.002(24)
		Li-O(8)	1.905(22)

B. Bond Angles (deg)

Fe(1)-P(1)-Fe(2)	73.7(1)	C(3)-Fe(2)-C(4)	105.5(7)
Fe(1)-P(2)-Fe(2)	74.0(1)	C(3)-Fe(2)-C(5)	99.4(7)
P(1)-Fe(1)-P(2)	81.2(1)	C(3)-Fe(2)-P(1)	102.2(7)
P(1)-Fe(2)-P(2)	79.6(1)	C(3)-Fe(2)-P(2)	108.2(7)
P(1)-Fe(1)-C(1-1)	155.4(3)	Fe(1)-C(1-1)-O(1-1)	124(1)
P(2)-Fe(1)-C(2)	152.2(3)	Fe(1)-C(1-1)-C(2-1)	120(1)
P(1)-Fe(1)-C(2)	94.7(3)		
P(2)-Fe(1)-C(1-1)	90.0(3)	C(2-1)-C(1-1)-O(1-1)	116(1)
C(2)-Fe(1)-C(1-1)	82.4(7)		
		Fe(1)-C(1)-O(1)	175(1)
C(1)-Fe(1)-C(1-1)	103.4(7)	Fe(1)-C(2)-O(2)	178(1)
		Fe(2)-C(3)-O(3)	176(1)
C(1)-Fe(1)-C(2)	104.2(7)	Fe(2)-C(4)-O(4)	177(1)
C(1)-Fe(1)-P(1)	101.0(3)	Fe(2)-C(5)-O(5)	176(1)
C(1)-Fe(1)-P(2)	103.6(3)		
P(1)-Fe(2)-C(5)	158.2(3)	O(1-1)-Li-O(6)	111(2)
P(2)-Fe(2)-C(4)	145.8(3)	O(1-1)-Li-O(7)	108(2)
P(1)-Fe(2)-C(4)	87.8(3)	O(1-1)-Li-O(8)	111(2)
P(2)-Fe(2)-C(5)	91.5(3)	O(6)-Li-O(7)	103(2)
C(4)-Fe(2)-C(5)	88.6(7)	O(6)-Li-O(8)	111(2)
		O(7)-Li-O(8)	113(2)

It is apparent from the above crystallographic data that the ion-pair interactions between alkali metal ions and the more negatively charged acyl oxygen atoms are considerably stronger than those between alkali metal ions and the carbonyl

Table IX. Least-Squares Planes for $[Li(C_4H_8O)_3]^+[Fe_2(CO)_5(C(O)Ph)(\mu_2\text{-}PPh_2)_2]^-$

A. Equations Defining the Least-Squares Planes[a]

plane I, through Fe(1), Fe(2), C(1-1)
$$-0.6177X - 0.7620Y - 0.1946Z + 5.9147 = 0$$
plane II, through C(1-1), C(2-1), O(1-1)
$$0.8397X + 0.5430Y - 0.0094Z - 4.8835 = 0$$
plane III, through P(1), P(2), C(1-1), C(2)
$$0.4411X - 0.7892Y - 0.4272Z + 4.0601 = 0$$
plane IV, through P(1), P(2), C(4), C(5)
$$0.4755X + 0.3218Y - 0.8187Z + 1.3390 = 0$$

B. Perpendicular Distances (Å) of Some Atoms from the Designated Planes

	I	II	III	IV
Fe(1)	0	0.06	0.45	1.67
Fe(2)	0	−0.87	−1.72	−0.47
P(1)	−0.25	0.04	0.01	−0.09
P(2)	1.75	−2.05	−0.01	0.09
C(1)	0.67	0.01	2.18	2.20
C(2)	−1.72	1.77	−0.01	2.69
C(3)	0.57	−1.83	−2.37	−2.20
C(4)	−2.90	0.72	−2.60	0.11
C(5)	0.05	−1.28	−2.81	−0.10
C(1-1)	0	0	0.01	2.92
C(2-1)	0.46	0	1.14	4.06
O(1-1)	−0.39	0	−1.13	2.85
Li	−1.41	0.67	−2.44	3.74

C. Angles (deg) between Normals to the Planes

	I	II	III	IV
I		158	66	112
II			93	54
III				72

[a] The equations of the planes are given in an orthogonal ångstrom coordinate system (X, Y, Z) which is related to the fractional unit cell coordinate system (x, y, z) as follows: $X = xa + zc\cos\beta$, $Y = yb$, $Z = zc\sin\beta$.

oxygen atoms. A similar tight-ion association is expected in solution for acyl metal carbonyl anions containing alkali metal ions in accord with previous interpretations[7,9b] of the solution structures of such species.

The crystallographic indication of a tighter Li^+–O(acyl) ion pair than Na^+–O(acyl) ion pair is consistent with the smaller, less charge-diffuse Li^+ ion producing a much larger electrostatic field strength and hence a greater charge-polarization effect on an acyl oxygen atom.

Experimental support for the much greater contact ion pairing of the Li^+ ion than the Na^+ ion to the acyl oxygen atom relative to the $[(Ph_3P)_2N]^+$ ion is given by the IR spectra of the three salts in THF solution exhibiting a much lower acyl carbonyl frequency for the lithium salt (1545 cm^{-1}) than that for the sodium salt (1570 cm^{-1}) compared to the bis(triphenylphosphine)iminium salt (1587 cm^{-1}).[2,6] This same ion-pairing trend was previously noted by Fischer and Kiener[4c] in the KBr-pellet IR spectra of the $[Fe(CO)_4(C(O)R)]^-$ monoanions (R = Ph, Me) as the lithium and $[NMe_4]^+$ salts. Considerably lower acyl carbonyl frequencies of 1519 and 1490 cm^{-1} were observed by them for the acetyl and benzoyl monoanions, respectively, of the lithium salts than those of 1584 and 1551 cm^{-1} for the acetyl and benzoyl monoanions, respectively, of the tetramethylammonium salts, which should have relatively weak ion pairing via N–H···O(acyl) hydrogen bonding.

The formation of the (metal–metal)-bonded acyl monoanions from the prior reduction of the (metal–metal)-bonded $Fe_2(CO)_6(\mu_2\text{-}PPh_2)_2$[24] to the (metal–metal)-nonbonded $[Fe_2(CO)_6(\mu_2\text{-}PPh_2)_2]^{2-}$ dianion[3] followed by reaction with an alkyl halide or tosylate is considered[2,6] most likely to proceed through an intermediate (metal–metal)-nonbonded alkyl monoanion (unisolated as yet) with Fe–Fe bond formation apparently being a large part of the driving force for alkyl interconversion to an acyl ligand. This mechanism is unusual in that rearrangement of alkyl to acyl metal complexes usually takes place in the presence of an external electron-donating ligand which fills the vacant coordination site. The observed ion pairing in the solid state for the lithium and sodium salts points to the rate of alkyl–acyl migratory insertion being highly dependent upon the nature of the cation, as previously found by Collman et al.[7] in the preparation of the acyl $[Fe(CO)_3L(C(O)R)]^-$ monoanions from alkyl $[Fe(CO)_4R]^-$ monoanions. This process in which the other adjacent iron atom allows internal Fe–Fe bond formation upon alkyl migration without direct interaction with the resulting acyl ligand bears a formal relationship to the oxidative addition of H_2 to the (Ir(I)–Ir(I))-nonbonded $Ir_2(CO)_4(\mu_2\text{-}SPh)_2$ dimer[44] in which a hydrogen atom becomes attached to each iridium with concomitant formation of an electron-pair Ir–Ir bond being part of the driving force for the reaction.

Acknowledgments. We are pleased to acknowledge support of this research by the National Science Foundation (CHE 75-17018) to J.P.C., by the National Science Foundation (PCM 75-17105) to K.O.H., and by the National Science Foundation (CHE 77-24309) to L.F.D. K.O.H. acknowledges the Alfred P. Sloan Foundation for a fellowship (1976-1978). We are also indebted to Dr. R. G. Finke, Mr. W. H. Armstrong, Dr. M. A. Bobrick, and Mr. A. M. Madonik of Stanford University and to Mr. Edward J. Wucherer and Mr. Don M. Washecheck of the University of Wisconsin-Madison for their special assistance in various parts of this work.

Supplementary Material Available: A listing of the observed and calculated structure factors (18 pages). Ordering information is given on any current masthead page.

References and Notes

(1) (a) University of Wisconsin—Madison; (b) Stanford University; (c) Eastman Kodak Co., Rochester, N.Y.
(2) J. P. Collman, R. K. Rothrock, R. G. Finke, and F. Rose-Munch, *J. Am. Chem. Soc.*, **99**, 7381 (1977).
(3) R. E. Ginsburg, R. K. Rothrock, R. G. Finke, J. P. Collman, and L. F. Dahl, *J. Am. Chem. Soc.*, in press.
(4) (a) P. F. Lindley and O. S. Mills, *J. Chem. Soc. A*, 1279 (1969); (b) E. O. Fischer, V. Kiener, D. St. P. Bunbury, E. Frank, P. F. Lindley, and O. S. Mills, *Chem. Commun.*, 1378 (1968); (c) E. O. Fischer and V. Kiener, *J. Organomet. Chem.*, **23**, 215 (1970).
(5) (a) J. R. Blickensderfer, C. B. Knobler, and H. D. Kaesz, *J. Am. Chem. Soc.*, **97**, 2686 (1975); (b) J. R. Blickensderfer and H. D. Kaesz, *ibid.*, **97**, 2681 (1975).
(6) (a) R. K. Rothrock, Ph.D. Thesis, Stanford University, 1978; (b) R. K. Rothrock and J. P. Collman, unpublished work.
(7) J. P. Collman, J. N. Cawse, and J. I. Brauman, *J. Am. Chem. Soc.*, **94**, 5905 (1972).
(8) (a) W. F. Edgell in "Ions and Ion Pairs in Organic Reactions", Vol. I, M. Szwarc, Ed., Wiley, New York, 1972, and references cited therein; (b) W. F. Edgell, J. Lyford IV, A. Barbetta, and C. I. Jose, *J. Am. Chem. Soc.*, **93**, 6403 (1971); (c) W. F. Edgell and J. Lyford IV, *ibid.*, **93**, 6407 (1971); (d) W. F. Edgell and N. Pauuwe, *Chem. Commun.*, 284 (1969).
(9) (a) C. D. Pribula and T. L. Brown, *J. Organomet. Chem.*, **71**, 415 (1974); (b) M. Y. Darensbourg and D. Burns, *Inorg. Chem.*, **13**, 2970 (1974); (c) D. J. Darensbourg, H. H. Nelson, III, and C. L. Hyde, *ibid.*, **13**, 2135 (1974); (d) M. Y. Darensbourg, D. J. Darensbourg, D. Burns, and D. A. Drew, *J. Am. Chem. Soc.*, **98**, 3127 (1976); (e) K. H. Pannell and D. Jackson, *ibid.*, **98**, 4443 (1976).
(10) J. P. Collman, R. G. Finke, J. N. Cawse, and J. I. Brauman, *J. Am. Chem. Soc.*, **99**, 2516 (1977).
(11) (a) H. B. Chin and R. Bau, *J. Am. Chem. Soc.*, **98**, 2434 (1976); (b) R. G. Teller, R. G. Finke, J. P. Collman, H. B. Chin, and R. Bau, *ibid.*, **99**, 1104 (1977).
(12) (a) J. C. Calabrese, FOBS, "A Fortran Diffractometer Data-Reduction Program", University of Wisconsin—Madison, 1972; (b) J. C. Calabrese, SORTMERGE, "A Data-Merging and Decay-Correction Program", Ph.D. Thesis (Appendix I), University of Wisconsin—Madison, 1971; (c) J. F. Blount, DEAR, "An Absorption-Correction Program", 1965; (d) J. C. Calabrese, PHASE, Ph.D. Thesis (Appendix II), University of Wisconsin—Madison, 1971; (e) J. C. Calabrese, MAP, "A Local Fortran Fourier Summation and Molecular Assemblage Program", 1972; (f) J. C. Calabrese, "A Crystallographic Variable Matrix Least-Squares Program", University of Wisconsin—Madison, 1972; (g) J. C. Calabrese, MIRAGE, Ph.D. Thesis (Ap-

pendix III), University of Wisconsin—Madison, 1971; (h) ORFLSR, "A Local Rigid-Body Least-Squares Program", adapted from the Busing–Martin–Levy ORFLS, ORNL-TM-305, Oak Ridge National Laboratory, Oak Ridge, Tenn., 1963; (i) W. R. Busing, K. O. Martin, and H. A. Levy, ORFFE, ORNL-TM-306, Oak Ridge National Laboratory, Oak Ridge, Tenn., 1964; (j) D. L. Smith, "A Least-Squares Planes Program", Ph.D. Thesis (Appendix IV), University of Wisconsin—Madison, 1962; (k) C. K. Johnson, ORTEP-II, 1970. All calculations were carried out on the Chemistry Department's Harris/7 computer at the University of Wisconsin—Madison.

(13) "International Tables for X-ray Crystallography", Vol. III, Kynoch Press, Birmingham, England, 1962, pp 161–165.

(14) In addition to FAME and a local data reduction program ENXDR, the programs used included full-matrix least squares, and Fourier programs; ABSCOR, a numerical method absorption correction program which applies a Gaussian grid to the crystal; a modified version of ORFFE (Busing and Levy's function and error program); and Johnson's ORTEP. All calculations were performed on a PDP 11/45 computer at Stanford University.

(15) (a) "International Tables for X-ray Crystallography", Vol. I, Kynoch Press, Birmingham, England, 1952, p 104; (b) *ibid.*, p 79; (c) *ibid.*, p 93.

(16) (a) For the space group $P2_122_1$ the general fourfold set of positions (4c) is x, y, z; $\bar{x}, y, \bar{z}$; $\frac{1}{2} + x, \bar{y}, \frac{1}{2} - z$; $\frac{1}{2} - x, \bar{y}, \frac{1}{2} + z$. The twofold set of special positions (2a) on twofold axes is 0, y, 0; $\frac{1}{2}, \bar{y}$, 0. (b) For the space group $P2_1/n$ the general fourfold set of positions (4e) is $\pm(x, y, z; \frac{1}{2} + x, \frac{1}{2} - y, \frac{1}{2} + z)$.

(17) Atomic scattering factors for neutral atoms were used.[18a,b] Anomalous dispersion corrections[18c,d] were applied to the scattering factors of the Fe and P atoms in the structural determinations of the $[(Ph_3P)_2N]^+$ and $(Li(THF)_3]^+$ salts and to the scattering factors of the Fe, P, and Na atoms in the structural determination of the $[Na(THF)_2]^+$ salt.

(18) (a) D. T. Cromer and J. B. Mann, *Acta Crystallogr., Sect. A*, **24**, 321 (1968); (b) R. F. Stewart, E. R. Davidson, and W. T. Simpson, *J. Chem. Phys.*, **42**, 3175 (1965); (c) D. T. Cromer and D. Liberman, *ibid.*, **53**, 1891 (1970); (d) ref 13, Vol. IV, 1974, p 149.

(19) The unweighted and weighted discrepancy factors used are $R_1(F) = [\Sigma||F_o| - |F_c||/\Sigma|F_o|] \times 100$ and $R_2(F) = [\Sigma w_i||F_o| - |F_c||^2/\Sigma w_i|F_o|^2]^{1/2} \times 100$. All least-squares refinements were based on the minimization of $\Sigma w_i||F_o| - |F_c||^2$ with individual weights of $w_i = 1/\sigma^2(F_o)$ assigned on the basis of the esd's[12a,20] of the observed structure factors.

(20) Cf. M. A. Bobrik, K. O. Hodgson, and R. H. Holm, *Inorg. Chem.*, **16**, 1851 (1977).

(21) E. R. Howells, D. C. Phillips, and D. Rogers, *Acta Crystallogr.*, **3**, 210 (1950).

(22) Cf. (a) L. B. Handy, J. K. Ruff, and L. F. Dahl, *J. Am. Chem. Soc.*, **92**, 7327 (1970), and references cited therein; (b) S. A. Goldfield and K. N. Raymond, *Inorg. Chem.*, **13**, 770 (1974); (c) G. Huttner and W. Gartzke, *Chem. Ber.*, **108**, 1373 (1975).

(23) (a) B. Metz, D. Moras, and R. Weiss, *Chem. Commun.*, 444 (1971); (b) D. Moras, B. Metz, and R. Weiss, *Acta Crystallogr., Sect. B*, **29**, 383 (1973); (c) *ibid.*, **29**, 388 (1973); (d) D. Moras and R. Weiss, *ibid.*, **29**, 396 (1973); (e) *ibid.*, **29**, 400 (1973); (f) F. J. Tehan, B. L. Barnett, and J. L. Dye, *J. Am. Chem. Soc.*, **96**, 7203 (1974); (g) D. G. Adolphson, J. D. Corbett, and D. J. Merryman, *ibid.*, **98**, 7234 (1976); (h) R. G. Teller, R. G. Finke, J. P. Collman, H. B. Chin, and R. Bau, *ibid.*, **99**, 1104 (1977).

(24) J. R. Huntsman, Ph.D. Thesis, University of Wisconsin—Madison, 1973.

(25) (a) L. F. Dahl, E. Rodulfo de Gil, and R. D. Feltham, *J. Am. Chem. Soc.*, **91**, 1653 (1969); (b) B. K. Teo, M. B. Hall, R. F. Fenske, and L. F. Dahl, *Inorg. Chem.*, **14**, 3103 (1975).

(26) An infrared spectrum[27] of $Fe_2(CO)_6(\mu_2\text{-}PPh_2)_2$ in hexane exhibits absorption bands in the carbonyl region at 2055 (m), 2052 (sh), 2018 (vs), 1994 (m), 1990 (sh), 1966 (s), and 1957 (w) cm^{-1}, whereas an infrared spectrum[6] of $[Li(THF)_3]^+[Fe_2(CO)_5(C(O)Ph)(\mu_2\text{-}PPh_2)_2]^-$ in THF has carbonyl bands at 2005 (s), 1953 (s), 1938 (s), 1920 (s), 1890 (m), and 1545 (w,br) cm^{-1}. The latter band is characteristic of the acyl ligand.

(27) B. E. Job, R. A. N. McLean, and D. T. Thompson, *Chem. Commun.*, 895 (1966).

(28) (a) Yu. A. Chapovskii, V. A. Semion, V. G. Andrianov, and Yu. T. Struchkov, *J. Struct. Chem.*, **9**, 990 (1968); (b) V. A. Semion and Yu. T. Struchkov, *ibid.*, **10**, 563 (1969).

(29) F. A. Cotton, B. A. Frenz, and A. Shaver, *Inorg. Chim. Acta*, 7, 161 (1973).

(30) H. Felkin, B. Meunier, C. Pascard, and T. Prange, *J. Organomet. Chem.*, **135**, 361 (1977).

(31) P. J. Van Vuuren, R. J. Fletterick, J. Meinwald, and R. E. Hughes, *J. Am. Chem. Soc.*, **94**, 4394 (1971).

(32) V. A. Semion and Yu. T. Struchkov, *J. Struct. Chem.*, **10**, 80 (1969).

(33) M. R. Churchill and J. P. Fennessey, *Inorg. Chem.*, **7**, 953 (1968).

(34) P. H. Bird and M. R. Churchill, *Inorg. Chem.*, **7**, 349 (1968).

(35) T. F. Block, R. F. Fenske, and C. P. Casey, *J. Am. Chem. Soc.*, **98**, 441 (1976).

(36) These MO calculations[35] were subsequently stated[37] to validate the $M^- - C^+$ ylide nature for this kind of metal carbene complex, in which the carbene carbon is best viewed as a carbocation stabilized by electron donation from the metal and from hetero substituents. An ESR study[37] of the radical monoanions generated by reduction of $M(CO)_5(C(OR)Ph)$ complexes (where M = Cr, Mo, W) was found to be in accord with the (Fenske–Hall)-type calculations[35,37] which predicted that the unpaired electron in $[Cr(CO)_5(C(OMe)Ph)]^-$ anion resides predominantly on the carbene ligand.

(37) P. J. Krusic, U. Klabunde, C. P. Casey, and T. F. Block, *J. Am. Chem. Soc.*, **98**, 2015 (1976).

(38) Alkylation reactions of $[trans\text{-}Fe(CO)_3L(C(O)R)]^-Li^+$ (where L = CO, PPh_3, $P(n\text{-}Bu)_3$, $P(OMe)_3$, and $P(OPh)_3$, and R = Ph, Me, and benzyl) with alkoxonium salts (viz., $[THFMe]^+[SO_3F]^-$ and $[Et_3O]^+[BF_4]^-$) were shown by Conder and Darensbourg[39] to produce iron carbene complexes by exclusive reaction at the acyl oxygen atom.

(39) H. L. Conder and M. Y. Darensbourg, *Inorg. Chem.*, **13**, 506 (1974).

(40) This assertion is in accord with the three O(THF)–Li–O(1–1) angles of 108 (2), 111 (2), and 111 (2)° corresponding closely to a regular tetrahedral angle of 109.5°.

(41) Y. Tanimoto, H. Kobayashi, S. Nagakura, and Y. Saito, *Acta Crystallogr., Sect. B*, **29**, 1822 (1973).

(42) Cf. (a) F. A. Cotton and C. M. Lukehart, *Prog. Inorg. Chem.*, **16**, 487 1972; (b) D. J. Cardin, B. Cetinkaya, and M. F. Lappert, *Chem. Rev.*, **72**, 545 (1972); (c) D. J. Cardin, B. Cetinkaya, M. J. Doyle, and M. F. Lappert, *Chem. Soc. Rev.*, **2**, 99 (1973); (d) G. Huttner and D. Regler, *Chem. Ber.*, **105**, 1230 (1972).

(43) M. R. Truter, *Struct. Bonding, (Berlin)*, **16**, 71 (1973).

(44) R. Poilblanc, *Nouveau J. Chem.*, **2**, 145 (1978).